DEVELOPMENT OF CATALYST SUPPORT MATERIAL FROM

PINDIGA BENTONITIC CLAY

BY

Nurudeen Salahudeen

Department of Chemical Engineering,

Ahmadu Bello University, Zaria, Nigeria.

February, 2012

DEVELOPMENT OF CATALYST SUPPORT MATERIAL FROM PINDIGA BENTONITIC CLAY

BY

Nurudeen Salahudeen
MSc/ENG/2192/2009-10

A Thesis submitted to the School of Postgraduate Studies,
Ahmadu Bello University, Zaria

In partial fulfillment of the requirements for the award of
Masters Degree in Chemical Engineering.

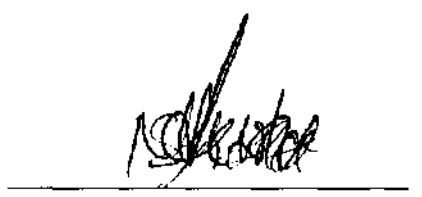
Department of Chemical Engineering,
Ahmadu Bello University, Zaria, Nigeria.

February, 2012

DECLARATION

I, Nurudeen Salahudeen hereby declare that the work in this thesis titled "Development of Catalyst Support Material from Pindiga Bentonitic Clay" was performed by me in the Department of Chemical Engineering, Ahmadu Bello University, Zaria, under the supervision of Prof. A. S. Ahmed and Dr. C. S. Ajinomoh of the Department of Chemical Engineering and Dr. H. Hamza of the Department of Geology. ABU, Zaria.

The information derived from the literature has been duly acknowledged in the text and a list of reference provided. No part of this work has been presented for another degree or diploma at any institution.



Signature

01/03/2012

Date

CERTIFICATION

This thesis entitled "Development of Catalyst Support Material from Pindiga Bentonitic Clay" meets the regulations governing the award of the degree of Master of Science (MSc) of the Ahmadu Bello University, and is approved for its contribution to knowledge and literary presentation.

Chairman, Supervisory Committee Prof. A. S. Ahmed	01/03/2012 Date
Member, Supervisory Committee Dr. C. S. Ajinomoh	02/03/12 Date
Head, Dept. of Chemical Engineering Dr. I. A Mohammed-Dabo	2/3/12 Date
Dean, School of Postgraduate Studies Prof. Adebayo. A. Joshua	16 APR 2012 Date

DEDICATION

This project work is dedicated to my most beloved, my mentor, my model, my leader and prophet, the best of mankind, son of Abdullah, Prophet Mohammad (S.A.W).

ACKNOWLEDGEMENT

All praises and glorifications are due to Allah (S.A.W) the creator and sustenance of the universe. He created the man and taught him what he knew not. To Him alone belong all attributes of perfection.

I acknowledge the immense courage and invaluable support of my parents in making my pursuit of education a reality. Indeed, I will always live to remember and gratify your role in my life. I say, may Allah reward you both with paradise.

I fully acknowledge the great role of the Petroleum Technology Development Fund (PTDF) Professorial Chair in Chemical Engineering, ABU, Zaria, for funding this research work.

My invaluable appreciation and acknowledgement goes to my learned Professor, my able supervisor, Prof. A. S. Ahmed, for his immeasurable courage and tireless supervision. Your sea of knowledge has magnanimously being an aid to the realization of this work.

In full measure, I also acknowledge the immense contribution of my minor Supervisors, Dr. C. S. Ajinomoh and Dr. H. Hamza. Your tireless contribution is fully appreciated.

My acknowledgement cannot be complete without expressing my profound appreciation to some individuals who have also contributed intellectually in realization of this work: Dr. I. A Mohammed-Dabo, Dr. B. O. Aderemi, Dr. Muktar Bello, Dr. S. M. Waziri, Dr. Mohammed Dauda, Mr. O. A. Ajayi, and all other academic and non academic staff of Chemical Engineering Department, Ahmadu Bello University, Zaria. I say thank you all for your contributions to the success of this work.

ABSTRACT

Catalyst support material was developed from Pindiga bentonitic clay using heat and acid treatment. Raw Pindiga elay was beneficiated using the wet method. The beneficiated clay was calcined at temperatures of 700°C, 750°C, and 800°C. Thereafter, the calcined clay samples were activated by acidifying with sulphuric acid, using wet acidification method at 95°C and dry acidification method at room temperature. The raw, beneficiated and acid treated clay samples were characterized using XRD, XRF and BET techniques. The XRD and XRF characterization results showed that the clay developed higher purity during beneficiation, calcinations and acidification as reflected by the decrease in organic impurities in form of carbon and graphite and reduction in quartz and soluble salts. The raw clay sample had very high iron impurity of up to 26.54 wt%. Only slight reduction in the iron content was observed after beneficiation and calcination but after acidification a reasonable reduction in the iron content was observed bringing the value to 12.80 wt% for 800°C calcined and wet acidified sample, and 15.34 wt% for 700°C calcined and wet acidified sample. Also, the BET characterization results showed that the clay developed larger surface area; the surface area of the raw clay which was 26.35 m7g increased to 43.81 m^2/g after beneficiation, and to 97.31, 99.32 and 139.59 m^2/g after calcination at 700°C, 750°C, and 800°C respectively. The surface area further increased to 191.41 and 270.44 m^2/g after wet acidification of the 700°C, and 800°C calcined samples respectively. The largest surface area values of 364.73 and 404.48 m^2/g were obtained for the 700°C, and 800°C calcined and dry acidified samples respectively.

Based on the surface area, the materials calcined and acidified can be considered as suitable for catalyst support, literature values being between 150 and 350 m^2/g for commercial montmorillonite clay suppors. The sample calcined at 800°C and wet acidified was considered the best support material on the basis of its lowest iron content of 12.80 wt% and high surface area of 270.44 m^2/g.

TABLE OF CONTENTS

CONTENT	PAGE
Title Page	i
Declaration	ii
Certification	iii
Dedication	iv
Acknowledgement	v
Abstract	vi
Table of Contents	vii
List of Tables	x
List of Figures	xi
List of Abbreviations and Symbols	xii
CHAPTER 1: INTRODUCTION	1
1.1 Research Problem	2
1.2 Research Aim	2
1.3 Research Objectives	2
1.4 Scope of the Research	3
1.5 Research Justification	3
CHAPTER 2: LITERATURE REVIEW	4
2.1 Clay	4
2.2 Clay Formation	5
2.3 Classification of Clay	5
2.4 Kaolinite	6

2.5	Montmorillonite	7
2.6	Bentonite	8
2.7	Classification of Bentonite	9
	2.7.1 Sodium bentonite	9
	2.7.2 Calcium bentonite	10
2.8	Thermal Stability of Bentonite Clay	10
2.9	Uses of Clay	11
	2.9.1 Clay as a building material	12
	2.9.2 Medical and agricultural uses	12
	2.9.3 Industrial uses of clay	13
2.10	Clay Structure	13
2.11	Relevance of Clay in the Petroleum Industry	17
2.12	Catalysis and Catalyst Support	17
	2.12.1 Choice of support material	19
	2.12.2 Homogeneous catalysis	21
	2.12.3 Heterogeneous catalysis	22
2.13	Catalytic Cracking	23
2.14	Acid Activation of Clay	24
2.15	Calcination of Clay	25
2.16	BET Adsorption Isotherm	26
2.17	X-ray Diffraction	28
2.18	X-ray Fluorescence	30
2.19	Zeolite Catalyst	33

CHAPTER 3: MATERIAL EQUIPMENT AND METHODOLOGY 34

3.1 Materials and Equipment 34

3.1.1 List of materials 34

3.1.2 List of apparatus 35

3.1.3 List of equipment 35

3.2 Experimental Procedure 36

3.2.1 Raw material collection 36

3.2.2 Beneficiation 37

3.2.3 Clay calcination 38

3.2.4 Clay activation 38

3.2.5 Determination of surface area 39

3.2.6 Characterization of clay samples 40

CHAPTER 4: RESULTS AND DISCUSSION 42

4.1 Determination of Physical Properties 42

4.2 Determination of Surface Area 43

4.3 Mineral Composition 45

4.4 Chemical Composition 48

CHAPTER 5: CONCLUSIONS AND RECOMMENDATIONS 51

5.1 Conclusions 51

5.2 Recommendations 53

REFERENCES 54

APPENDIX 57

LIST OF TABLES

Table No.	Title	Page No.
2.1	Classification of Typical Support Materials.	20
2.2	Comparism Between Alumina and Clay	21
4.1	Results of Density and the pH Tests	42
4.2	BET Results Obtained for the Standards Used for Correction Factor	44
4.3	Summary Result for Surface Area of Each Sample	44
4.4	Chemical Composition of the Raw, Beneficiated and Treated Clay	48

LIST OF FIGURES

Figure No.	Title	Page No.
2.1	Corn Flake like Shape of Montmorillonite Crystalline Structure	8
2.2	Differential Thermal Analysis Pattern of a Typical Natural Bentonite	11
2.3	Structural Illustration of the Si Tetrahedron Primary Building Unit	14
2.4	Structural Illustration of the Al Octahedron Primary Building Unit	14
2.5	Illustration of Structural Regrouping of Si PBU to Form SBU	15
2.6	Illustration of Structural Regrouping of Al PBU to Form SBU	15
2.7	Illustration of Structural Architectural Form in 1:1 Type of Clay Structure	16
2.8	Illustration of Structural Architectural Form in 1:2 Type of Clay Structure	16
2.9	Diagrammatic View of the Swelling Nature of 1:2 Clay Structure	17
2.10	Crystal Structure of Alumina	21
2.11	Bragg's Relation Between the Incident and Diffracted Beams	29
2.12	Pictorial Illustration of Zeolite Crystal Structure	33
3.1	Flow diagram of the raw clay beneficiation process	37
3.2	Flow diagram of the clay calcination and acidification processes	39
4.1	XRD Patterns for the Various Samples of Pindiga Clay	47

LIST OF ABREVIATIONS AND SYMBOLS

Abbreviations/Symbol	Meaning
atm	Atmosphere
DSC	Differential Scanning Calorimeter
DTA	Differential Thermal Analysis
K	Kelvin
L.O.I	Loss on Ignition
m	Meter
rpm	Revolution per minute
XRD	X-ray diffraction
XRF	X-ray fluorescence
θ	Angle
ρ	Density

CHAPTER 1

INTRODUCTION

The global rapid growing demand for energy sources especially from fuels, since the discovery of petroleum, had compelled chemical and petroleum engineers to embark on research on how to increase conversion capacity of crude oil to more useful light ends, especially gasoline. This quest resulted to the petroleum cracking technology. Cracking means the breaking down of large hydrocarbon molecules into smaller and more useful fractions. This can be done by the thermal or catalytic method.

The catalytic method, which entails cracking in the presence of a suitable catalyst produces an improvement in product yield and quality over the earlier simple thermal cracking which was employed via high temperature. Hence, the catalytic method is the method adopted in virtually all modern petroleum refineries, it is applied as fluidized catalytic cracking (FCC) process.

The catalysts used in the catalytic cracking of petroleum are mainly zeolite catalysts which consist of; zeolite active ingredient and catalyst support. FCC catalyst support can be made of alumina or clay, they are incorporated in the design of the catalyst to ensure optimal and most stable geometry of the overall catalyst, to optimize the economy and efficiency of the catalyst among other benefits.

For the choice of support material, the clay has greater economic advantages over alumina due to the fact that clay is cheaper and occurs naturally. The two major clays used as support material for catalysts are kaolin and bentonite. Kaolin has advantage of low heavy metal contamination;

especially iron (Fe), which has detrimental effect of poisoning on the catalyst's active sites. However, kaolin has the limitation of being thermally unstable at temperatures above 500°C where it undergoes phase change to form metakaolin and other phase transformations with further heating. Whereas bentonitic clay is stable up to 800°C (Sand, 1960).

This research work is focused on production of catalyst support for fluidized catalytic cracking catalysts FCC, from Pindiga bentonitic clay minerals.

1.1 RESEARCH PROBLEM

Nigeria is blessed abundantly with mineral resources, among which are clay minerals. These resources have not been extensively exploited, rather in many cases they are left wasted. Hence, in order to exploit and improve the commercial value of Pindiga bentonitic clay, it is necessary to investigate its suitability for industrial uses, including its use as a support material for FCC zeolite catalyst.

1.2 RESEARCH AIM

To develop a catalyst support material from Pindiga bentonitic clay.

1.3 RESEARCH OBJECTIVES

1. To study the effect of beneficiation on the mineral and chemical compositions, and the specific surface area characteristic of raw Pindiga bentonitic clay mineral obtained from its formation.

2. To investigate the effect of thermal and mineral acid treatments on Pindiga bentonitic clay with respect to its chemical and mineral compositions, and specific surface area characteristic.

1.4 SCOPE OF THE RESEARCH

The scope of this research work covered collection and variable treatments of raw Pindiga clay to enhance its suitability for application as support material for FCC zeolite catalyst, by adopting;

i. Wet beneficiation.

ii. Heat treatment at calcination levels.

iii. Acid treatment with sulphuric acid by dry and wet methods

iv. Characterization of the raw and treated clay using:

a. X-ray Diffraction technique (XRD).

b. BET technique.

c. X-ray fluorescence technique (XRF)

1.5 RESEARCH JUSTIFICATION

1. This will lead to formulation and production of a local zeolite catalyst for use in the Nigerian oil and gas industry.
2. Local catalyst factories could be established, hence large job opportunities would emerge.
3. These would save foreign exchange earning.

CHAPTER 2

LITERATURE REVIEW

2.1 CLAY

Clay minerals are layered-type hydrous aluminosilicate minerals which are major products of weathering processes of aluminosilicate rocks. Complete weathering of volcanic igneous rocks, especially feldspars, lead to clay mineral formation. Clay minerals never occur as large crystals but are usually found in what are known as "muds"; the predominant clay particles are often less than one micrometer ($<10^{-4}$ cm) in diameter, placing them in the colloidal size range. Because of their small particle size, clays have large surface area to mass ratios. Clays have structures similar to the micas and therefore form flat tetrahedral, octahedral or hexagonal sheets which lay on each other in a certain pattern which determine their classification. (Anonymous[(A)], 2011).

In mineral composition they consist of aluminum phyllosilicates with variable amounts of physically and chemically combined water and traces of metallic impurities like; iron; magnesium; alkali metals; alkaline earths and other cations in their oxide forms. It also consist of other impurities of sulfate or/and carbonate salts which are generally lost together with the combined water as lost on ignition (LOI) when the clay is heated to high degree. Clays are distinguished from other fine-grained soils by differences in size and mineralogy. Silts, which are fine-grained soils that do not include clay minerals tend to have larger particle sizes than clays, but there is some overlap in both particle size and other physical properties, and there are many naturally occurring deposits which include both silts and clays. The distinction between silt and clay varies by discipline. Geologists and soil scientists usually consider the separation to occur at a particle size of 2 μm (clays being finer than silts), sedimentologists often use 4-5 μm,

and colloid chemists use 1 µm. Geotechnical engineers distinguish between silts and clays based on the plasticity properties of the soil, as measured by the soils' Atterberg Limits. ISO 14688 grades clay particles as being smaller than 2 µm and silts are larger (Anonymous[A], 2011).

2.2 CLAY FORMATION

Clay minerals are typically formed over long periods of time by the gradual chemical weathering of rocks, usually silicate-bearing, by low concentrations of carbonic acid and other diluted solvents. These solvents, usually acidic, migrate through the weathering rock after leaching through upper weathered layers. In addition to the weathering process, some clay minerals are formed by hydrothermal activity. Clay deposits may be formed as result of residual deposits in soil, but thick deposits usually are formed as the result of a secondary sedimentary deposition process after they have been eroded and transported from their original location of formation. Clay deposits are typically associated with very low energy depositional environments such as large lakes and marine deposits. Primary clays, also known as kaolins, are located at the site of formation. Secondary clay deposits have been moved by erosion and water from their primary location. (Anonymous[A], 2011).

2.3 CLASSIFICATION OF CLAY

There are three or four main groups of clays (Anonymous[A], 2011).:

- Kaolinite Group:

  This include kaolinite, dickite, halloysite, and nacrite minerals. The chemical formular is $Al_2Si_2O_5(OH)_4$. This group of clay minerals is regarded as the 1:1 structural class.

- Montmorillonite:

  Members in this group include dioctahedral smectites such as montmorillonite and nontronite and trioctahedral smectites for example saponite. Their general chemical formular is $(Na,Ca)_{0.33}(Al,Mg)_2(Si_4O_{10})(OH)_2 \cdot nH_2O$

- Chlorite group:

  This group includes a wide variety of similar minerals with considerable chemical variation. Chlorites are not always considered as clay, sometimes being classified as a separate group within the phyllosilicates. There are approximately 30 different types of "pure" clays in these categories, but most "natural" clays are mixtures of these different types, along with other weathered minerals.

- Quick clay:

  This is a unique type of marine clay indigenous to the glaciated terrains of Norway, Canada, Northern Ireland, and Sweden. It is a highly sensitive clay, prone to liquefaction, which has been involved in several deadly landslides (Anonymous[A], 2011).

2.4 KAOLINITE

Kaolinite is a clay mineral, part of the group of industrial minerals, with the chemical composition $Al_2Si_2O_5(OH)_4$. It is a layered silicate mineral, with one tetrahedral sheet linked through oxygen atoms to one octahedral sheet of alumina octahedra. Rocks that are rich in kaolinite are known as china clay, white clay, or kaolin. Kaolinite has a low shrink-swell capacity and a low cation exchange capacity (1-15 meq/100g.) It is a soft, earthy, usually white

mineral (dioctahedral phyllosilicate clay), produced by the chemical weathering of aluminium silicate minerals like feldspar. In many parts of the world, it is colored pink-orange-red by iron oxide, giving it a distinct rust hue. Lighter concentrations yield white, yellow or light orange colours. Alternating layers are sometimes found, as at Providence Canyon State Park in Georgia, USA. Kaolin is used in ceramics, medicine, coated paper, as a food additive in toothpaste, as a light diffusing material in white incandescent light bulbs, and in cosmetics. It is generally the main component in porcelain. It is also used in paint to extend titanium dioxide (TiO_2) and modify gloss levels; in rubber for semi-reinforcing properties; and in adhesives to modify rheology (Anonymous[(A)], 2011).

2.5 MONTMORILLONITE

Montmorillonite is a very soft phyllosilicate mineral that typically forms in microscopic crystals, forming a clay. It is named after Montmorillon in France. Montmorillonite, a member of the Smectite family, is a 2:1 clay, meaning that it has 2 tetrahedral sheets sandwiching a central octahedral sheet. The particles are plate-shaped with an average diameter of approximately 1 micrometre. It is the main constituent of the volcanic ash weathering product. Chemically Montmorillonite is hydrated sodium calcium aluminum magnesium silicate hydroxide $(Na,Ca)_{0.33}(Al,Mg)_2(Si_4O_{10})(OH)_2 \cdot nH_2O$. Potassium, iron, and other cations are common substitutes; the exact ratio of cations varies with source. It often occurs intermixed with chlorite, muscovite, illite, cookeite and kaolinite. Montmorillonite has a crystalline structure which results in a "flake" particle shape that resembles a corn flake. These flakes are extremely small, ranging in long dimension from 10 micrometers to 0.01 micrometers (Figure 2.1) (aquatechnologies.com). Hundreds of such flakes aggregate to form a thin particle. One gram of

montmorillonite has a surface area of 750 m^2/g, nearly as much as the best activated carbon grains. Twelve grams have a surface area that covers an entire football field.

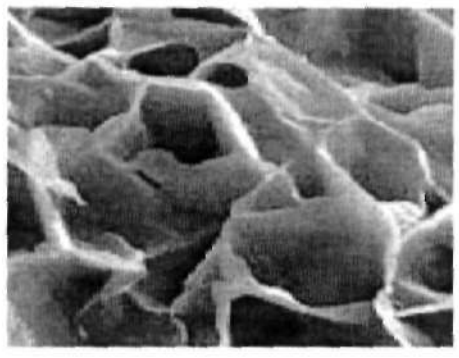


Figure 2.1: Corn flake like shape of montmorillonite crystalline structure (Anonymous[B], 2011).

2.6 BENTONITE

Bentonite is a dark-grey to dark-green absorbent aluminium phyllosilicate minerals composed of mostly Montmorillonite, with minor concentrations of cristobalite, zeolite, and quartz, among others. Bentonite usually forms from weathering of volcanic ash, most often in the presence of water. However, the term bentonite, as well as a similar clay called tonstein, has been used for clay beds of uncertain origin. In stratigraphy and tephrochronology, completely devitrified (weathered volcanic glass) ash-fall beds are commonly referred to as K-bentonites when the dominant clay species is illite. Much of bentonite's usefulness in the drilling and geotechnical engineering industry comes from its unique rheological properties. Relatively small quantities of bentonite suspended in water form a viscous, shear thinning material. Most often, bentonite suspensions are also thixotropic, although rare cases of rheopectic behavior have also been reported. At high enough concentrations (~60 grams of bentonite per litre of suspension), bentonite suspensions begin to take on the characteristics of a gel (a fluid with a minimum yield

strength required to make it move). For these reasons it is a common component of drilling mud used to curtail drilling fluid invasion by its propensity for aiding in the formation of mud cake. Bentonite can be used in cement, adhesives, ceramic bodies, and cat litter. Bentonite is also used as a binding agent in the manufacture of taconite pellets as used in the steelmaking industry. It also has medical and agricultural uses (Anonymous[C], 2011).

2.7 CLASSIFICATION OF BENTONITE

There are different types of bentonite, each named after the respective dominant element, such as potassium (K), sodium (Na), calcium (Ca), and aluminum (Al). Experts debate a number of nomenclatorial problems with the classification of bentonite clays. For industrial purposes, two main classes of bentonite exist: sodium and calcium bentonites (Anonymous[C], 2011).

2.7.1 Sodium Bentonite

Sodium bentonite expands when wet, absorbing as much as several times its dry mass in water. Because of its excellent colloidal properties, it is often used in drilling mud for oil and gas wells and for geotechnical and environmental investigations. The property of swelling also makes sodium bentonite useful as a sealant, especially for the sealing of subsurface disposal systems for spent nuclear fuel and for quarantining metal pollutants of groundwater. Similar uses include making slurry walls, waterproofing of below-grade walls, and forming other impermeable barriers, e.g., to seal off the annulus of a water well, to plug old wells, or to line the base of landfills to prevent migration of leachate. It is also used to form a barrier around newly planted trees to constrain root growth so as to prevent damage to nearby pipes, footpaths and other infrastructure (Anonymous[C], 2011).

2.7.2 Calcium Bentonite

Calcium bentonite is a useful adsorbent of ions in solution, as well as fats and oils, being a main active ingredient of fuller's earth, probably one of the earliest industrial cleaning agents. Calcium bentonite may be converted to sodium bentonite (termed sodium beneficiation or sodium activation) to exhibit many of sodium bentonite's properties by a process known as "ion exchange" (patented in 1935 by Germans U Hofmann and K Endell). In common usage, this means adding 5–10% of a soluble sodium salt such as sodium carbonate to wet bentonite, mixing well, and allowing time for the ion exchange to take place and water to remove the exchanged calcium. Some properties, such as viscosity and fluid loss of suspensions, of sodium-beneficiated calcium bentonite (or sodium-activated bentonite) may not be fully equivalent to those of natural sodium bentonite. For example, residual calcium carbonates (formed if exchanged cations are insufficiently removed) may result in inferior performance of the bentonite in geosynthetic liners (Anonymous[C], 2011).

2.8 THERMAL STABILITY OF BENTONITE CLAY

Figure 2.2 presents the DTA pattern of a natural Wyoming Bentonite, it can be seen from the pattern that the clay loses its physically combined water at about 50°C and completes at 150°C as shown by the first endothermic peak. Further heating resulted into loss of chemically combined water, from around 550°C to 700°C as shown by the second endothermic peak. Thus natural bentonic clay can be rendered thermally stable up to 700 - 800°C if preheated to 700 - 800°C to remove all chemically combined water.

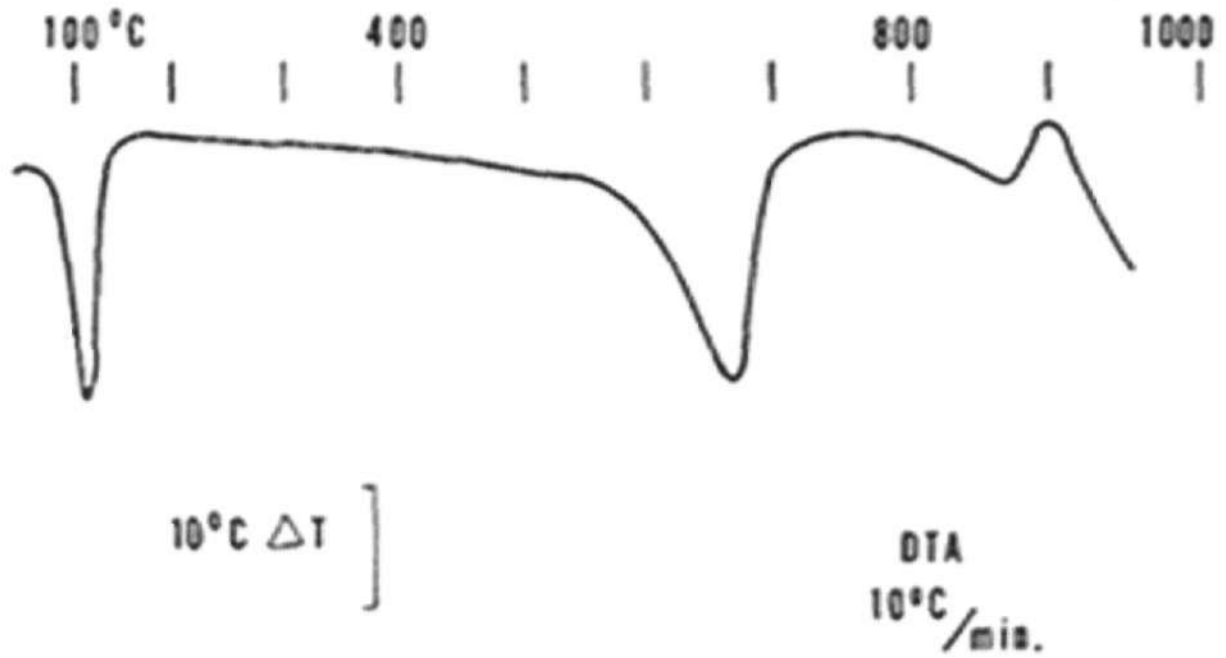


Figure 2.2: Differential thermal analysis pattern of a typical natural bentonite (Sand, 1960).

2.9 USES OF CLAY

Dry clay is normally much more stable than sand with regard to excavations. Clays exhibit plasticity when mixed with water in certain proportions. When dry, clay becomes firm and when fired in a kiln, permanent physical and chemical changes occur. These reactions, among other changes, cause the clay to be converted into a ceramic material. Because of these properties, clay is used for making pottery items, both utilitarian and decorative. Different types of clay, when used with different minerals and firing conditions, are used to produce earthenware, stoneware, and porcelain. Prehistoric humans discovered the useful properties of clay, and one of the earliest artifacts ever uncovered is a drinking vessel made of sun-dried clay. Depending on the content of the soil, clay can appear in various colors, from a dull gray to a deep orange-red. Clay tablets were used as the first known writing medium, inscribed with cuneiform script through the use of

89481

a blunt reed called a stylus. Clays sintered in fire were the first form of ceramic. Bricks, cooking pots, art objects, dishware, and even musical instruments such as the ocarina can all be shaped from clay before being fired. Until the late 20th century bentonite clay was widely used as a mold binder in the manufacture of sand castings. Clay, being relatively impermeable to water, is also used where natural seals are needed, such as in the cores of dams, or as a barrier in landfills against toxic seepage (lining the landfill, preferably in combination with geotextiles) (Anonymous[(A)], 2011).

2.9.1 Clay as a Building Material

Clay is one of the oldest building materials on Earth, among other ancient, naturally-occurring geologic materials such as stone and organic materials like wood. Between one-half and two-thirds of the world's population, in traditional societies as well as developed countries, still lives or works in a building made with clay as an essential part of its load-bearing structure. Also a primary ingredient in many natural building techniques, clay is used to create adobe, cob, cordwood, and rammed earth structures. And it is even the major starting material for the production of the modern cement (Anonymous[(A)], 2011).

2.9.2 Medical and Agricultural Uses

A traditional use of clay as medicine goes back to prehistoric times. An example is Armenian bole, which is used to soothe an upset stomach, similar to the way parrots (and later, humans) in South America originally used it. Kaolin clay and attapulgite have been used as anti-diarrheal medicines. A more recent and limited use is as a specially formulated spray applied to fruits, vegetables, and other vegetation to repel or deter codling moth damage, and at least for apples, to

prevent sun scald. A 2007 article in The Journal of Antimicrobial Chemotherapy found that certain iron-rich clay was effective in killing bacteria (Anonymous[A], 2011).

2.9.3 Industrial Uses of Clay

Clay is not left out in the modern technological advancement, it has been a key role player in the modern advancements in material science and technology, as it is being used as a raw material or additive for varieties of modern ceramics, refractories, hydrogels, polymers and composites materials, among others. Clay is also used in many industrial processes, such as paper making, cement production, and chemical filtering. Clay is also often used in the manufacture of pipes for smoking tobacco. Recent studies have investigated clay's absorption capacities in various industrial applications, such as the removal of heavy metals from waste water and air purification. And the discovery of its catalytic potentials has been a major land mark in its industrial application and economic importance (Anonymous[A], 2011).

2.10 CLAY STRUCTURE

Clay structures are fundamentally built from a structurally defined primary building units (PBU) The PBUs are formed by Si^{4+} in coordination with four oxygen atoms to form a two-dimensional tetrahedron, SiO_4 and Al^{6+} in coordination with six atoms of oxygen and hydrogen to form two-dimensional octahedron, AlH_3O_6 (Ferris, 2000).

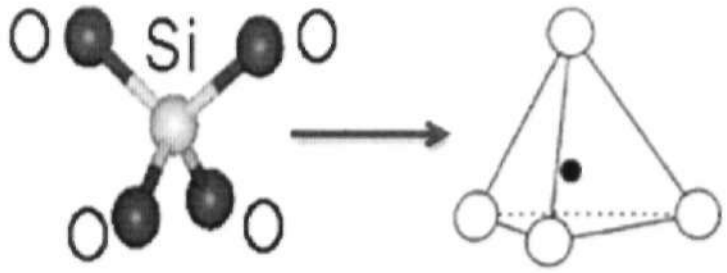


Figure 2.3: Structural illustration of the Si tetrahedron primary building unit (Ferris, 2000).

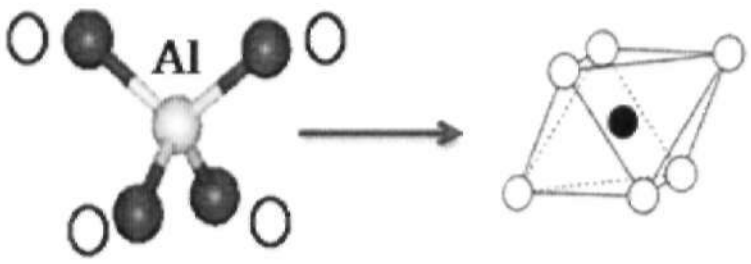


Figure 2.4: Structural illustration of the Al octahedron primary building unit (Ferris, 2000).

The Si PBUs are further regrouped in a specific fashion to form a hexagonal sheet of secondary building units (SBU). The PBU containing Si^{4+} are linked up by each tetrahedron sharing 3 of its vertex oxygen atoms with other tetrahedra resulting to coordination by six oxygen atoms to form a hexagonal SBU array in two-dimensions. The fourth vertex is not shared with another tetrahedron and all of the tetrahedra "point" in the same direction; i.e. all of the unshared vertices are on the same side of the sheet as can be seen in figure 2.3 above.

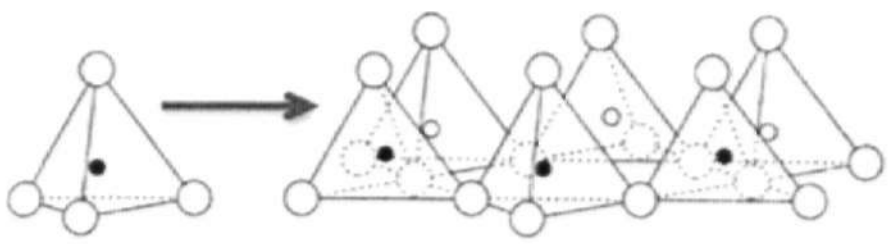


Figure 2.5: Illustration of structural regrouping of Si PBU to form SBU (Ferris, 2000).

The Al^{6+} PBUs are also regrouped to form an octahedral sheet of secondary building units (SBU) as can be seen in figure 2.6 below.

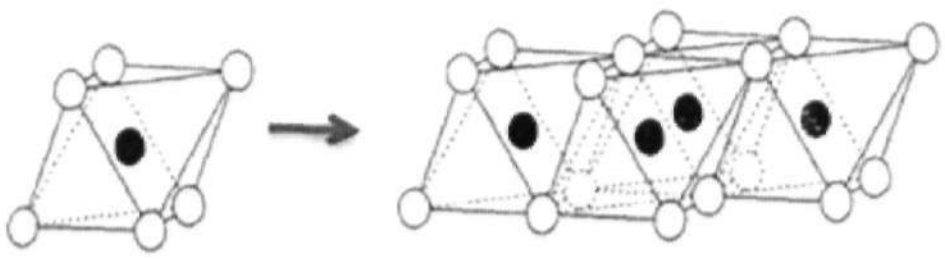


Figure 2.6: Illustration of structural regrouping of Al PBU to form SBU (Ferris, 2000).

The crystal structural architect of aluminosilicate clays consists of either two or three layers of SBU sheets which are spread upon each other in fashion that determines if the clay is a 1:1 or 1:2 structural type. In the 1:1 structural type, an aluminum-containing octahedron SBU sheet spreads on silicon-containing tetrahedron SBU sheet, examples include kaolinite and serpentine. While in 1:2, an aluminum-containing octahedron SBU sheet is sandwiched between two silicon-containing tetrahedron SBU sheets, examples include illite, smectite, attapulgite, motmorillonite, and chlorite (although chlorite has an external octahedral sheet often referred to as "brucite").

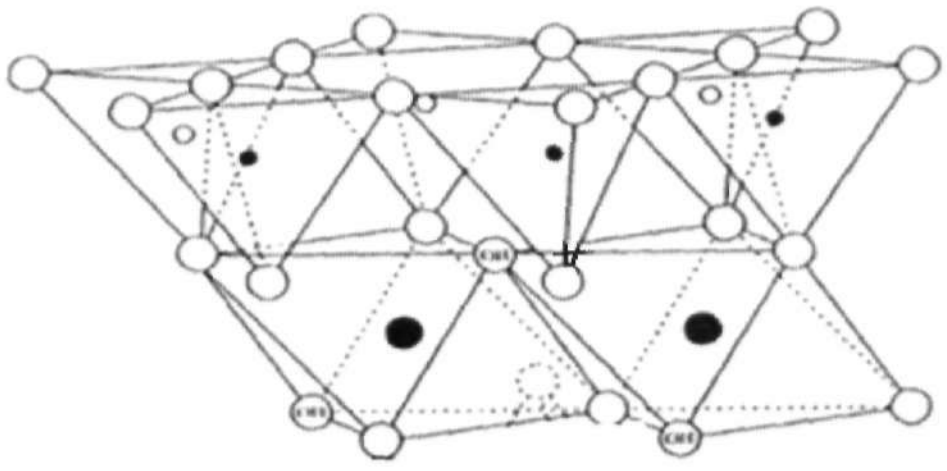


Figure 2.7: Illustration of structural architectural form in 1:1 type of clay structure (Ferris, 2000).

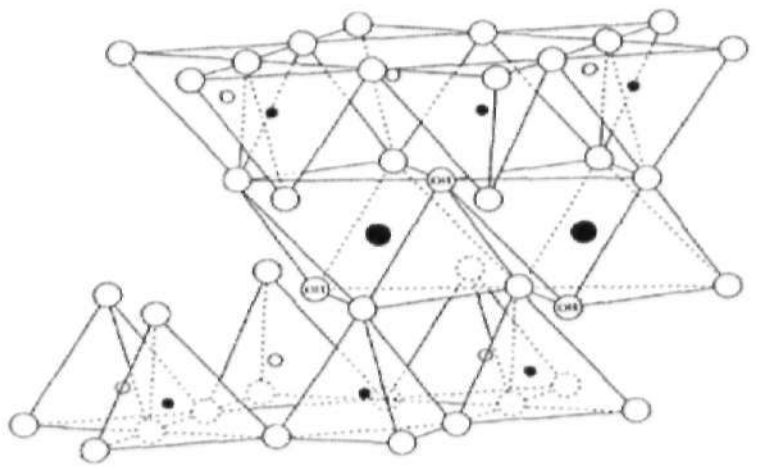


Figure 2.8: Illustration of structural architectural form in 1:2 type of clay structure (Ferris, 2000).

In the 1:2 structural type the O^{2-} at the apexes of the silica tetrahedra replaces the OH^- groups of the octahedral layer, and are shared between the layers. This three-layer grouping is referred to as a platelet. The platelets stack in various ways. Water is absorbed between the platelets, hence, clay of this type which are referred to as the swelling clay derived their name from this phenomenon. Due to the sharing between O^{2-} and OH^- there result in unsatisfied negative charge on the face of the clay platelet caused by structural substitutions or vacancies in the octahedral and/or tetrahedral layers. For example Mg^{2+} or another divalent cation may substitute for Al^{3+} in the octahedral layer, or Al^{3+} or Fe^{3+} may replace Si^{4+} in the tetrahedral layer. Cations such as Ca^{2+}, Mg^{2+}, and Na^+ are attracted to the spaces between the platelets due to the net negative charge on the "faces" of the platelets. These cations can be exchanged readily through washing.

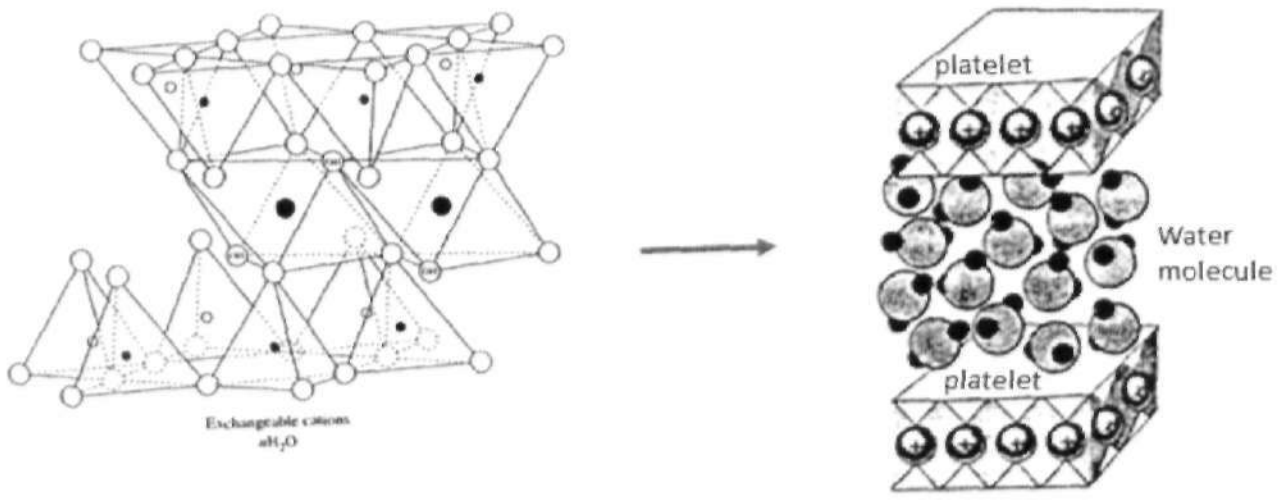


Figure 2.9: Diagrammatic view of the swelling nature of 1:2 clay structure (Ferris, 2000).

2.11 RELEVANCE OF CLAY IN THE PETROLEUM INDUSTRY

Clay is an indispensable material required by different processes in the Petroleum Industry, starting from the upstream to the down stream processes. In the upstream bentonite clay is used as the an excellent drilling mud in the mining exploration of a crude oil well. While in the down stream activated clays was used in the past as the major catalysts used in the FCC cracking process of heavier hydrocarbon fractions to lighter ends. However, in the modern petroleum refining technology the use of clay as FCC catalyst as been replaced by zeolite catalyst. Nevertheless, clay is still used as a catalyst support for the catalyst used in the same FCC unit (Grenall, 1949).

2.12 CATALYSIS AND CATALYST SUPPORT

A catalyst is a chemical substance that speeds up the rate of a chemical reaction, without participating in the reaction though it may undergo an intermediate chemical transformation or/and permanent physical change, it remains chemically unchanged at the end of the reaction.

Catalysts usually perform their role by affecting the selectivity of a particular reaction by increasing the reaction rate in that direction. Central to catalysis is the notion of the catalytic "site." It is defined as the catalytic center involved in the reaction steps. Catalysts usually consist of one or more active components imposed on surface of an oxidation material referred as catalyst support. Support material acting as building block for catalysts has many advantages such as: (Trimm, 1980).

1. Economics:

   (a) To reduce cost by extending an expensive catalyst.

2. Mechanical:

   (a) To give mechanical strength

   (b) To optimize bulk density

   (c) To provide a heat sink or a heat source

3. Chemical:

   (a) To dilute an overactive phase.

   (b) To pre-crack heavy hydrocarbons that are too large to pass through the zeolite pores by donating it proton to them.

   (c) To react with the catalyst either to improve specific activity or to minimise sintering

   (d) To accept or donate chemical entities, possibly via a spillover mechanism

4. Geometry:

    (a) To maximize surface area of the catalyst.

    (b) To optimize the porosity of the catalyst.

    (c) To optimize crystal and particle size.

    (d) To allow the catalyst particles adopt the most favourable configuration

    (e) Achieving a good dispersion of active components

5. Deactivation

    (a) To stabilize the catalyst against sintering

    (b) To minimize poisoning

2.12.1 Choice of Support Material

The catalytic performance of a catalyst depends on its different components, such as support and active metal. Usually, the behavior of the active phase is influenced by the type of support material; thus, it becomes necessary to select an optimum support material according to the criteria of interaction with active phases, acid-base properties (inertness), textural properties, stability, extrusion properties, and cost at commercial scale. In that a support material is required, in a perfect world, to fulfill all of the functions outlined in section 2.12, overall optimization can be complex and can lead to incompatible requirements. Thus, for example optimal porosity usually leads to a catalyst which is too weak mechanically. This is particularly important in that a major potential cause of catalyst failure is a result of mishandling during loading of the reactor. Before considering these factors individually, it is useful to consider briefly the type of materials that are used as supports. Since solid is largely inactive, a support is usually chosen for its

stability towards temperature over the range of operating conditions and for its surface and porosity. Generally, the support is not catalytically active over range of operating conditions, but if there is some small unwanted activity, this can be eliminated by, for example, selective poisoning. The most stable range of support includes such solids as alumina, magnesia, silicon carbide, and alumino-silicate; many naturally occurring materials belong to this last group, such as pumice, asbestos, calcined clay (e.g. bentonite, sepilite) and diatomaceous earth such as kieselguh. As result of their wide variation in structure, the solids offer wide range of surface area and porosity. (Trimm, 1980)

Table 2.1: Classification of some typical support materials (Trimm, 1980).

Low Surface Area (< 1 $m^2 g^{-1}$)		**High Surface Area (> 1 $m^2 g^{-1}$)**	
Non-porous	**Porous**	**Non-porous**	**Porous**
Ground glass Alumdum (α-Al_2O_3) Silicon carbide	Kieselguhr Pumice	Natural silica-alumina Carbon black Titania Zinc oxide	Natural clay Synthetic silica-alumina Alumina Magnesia Activated carbon Silica Asbestos

The most popular in application of these supports remains γ-alumina due to its high surface area high thermal stability, outstanding mechanical properties, and nature of interaction with the zeolite active phases. Though, clay, being a refractory material can also offer an excellent thermal and mechanical stability. Furthermore, its surface area can also be improved to approach or even exceed the surface area alumina if properly treated by calcination and/or chemical treatment. (Trimm, 1980).

Table 2.2: Comparism between properties of alumina and clay (Trimm, 1980)

PROPERTY	CLAY	ALUMINA
Stability	up to 900°C	≤ 1200°C
Melting point	2850°C	2977°C
Surface area	150 – 350 m^2g^{-1}	200 - 300 m^2g^{-1}

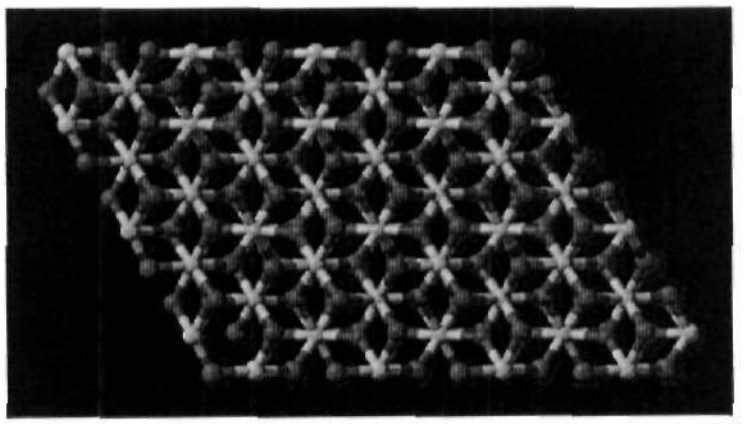


Figure 2.10: Crystal structure of alumina (Trimm, 1980).

2.12.2 Homogeneous Catalysis

In homogeneous catalysis the catalyst and reactants form a homogeneous system, for example, gas mixtures, or liquid solutions. The mechanism of the reaction is explained quite well by the theory of intermediate chemical compounds. By this theory, a catalyst forms an unstable reactive intermediate with a reactant. The activation energy of this process is lower than that of non-catalytic basic reaction. Subsequently, the intermediate decomposes or reacts with a new molecule of a reactant, freeing the catalyst in an unchanged form. These transformations are characterized by comparatively low activation energy (Erikh, 1988).

2.12.3 Heterogeneous Catalysis

In heterogeneous catalysis, the catalyst is most frequently in the solid phase, while the reactants are in the gaseous or vapour state. Cases are possible where the reactants and catalysts are immiscible liquids. The most popular catalytic processes for producing fuel in the petroleum-refining industry are catalytic cracking, isomerization, reforming, alkylation, and hydrocracking. In heterogeneous catalysis, all the changes and transformations of substances occur at the interface of the solid phase of the catalyst and the gas or vapour phase of the reactants and are associated considerably with the phenomenon of sorption. The process can be divided into the following five stages:

(1) Motion (diffusion) of the reacting molecules to the catalyst surface;

(2) Activated adsorption (chemisorption) of the reactant on the catalyst surface;

(3) A chemical reaction on the catalyst surface;

(4) Desorption (removal from the catalyst surface) of the reaction products;

(5) Diffusion of the products back to the gaseous stream.

The rate of the whole process is determined by that of the slowest stage. Here two cases are distinguished. If diffusion of the reactants and products proceed more rapidly than the catalytic reaction itself, the rate of the process depends completely on the composition and properties of the catalyst surface. Such a process is said to be kinetically controlled. Conversely, if diffusion proceeds at a slower rate than all the transformations on the catalyst surface occur, the overall rate of the reaction will be determined by the rate of diffusion. Such a process is said to be diffusion-controlled. The activation energy in heterogeneous catalytic reaction is lowered as a result of involved physiochemical processes characterizing the stage of activated adsorption (chemisorption). Chemisorption is the formation of a sufficiently strong mono-molecular layer of

the reactants on the surface of a catalyst. It proceeds at the expense of the valence forces of the catalyst, is in essence close to a real chemical reaction, and therefore results in appreciable weakening of the bonds in the reacting molecules.

The activated desorption of the reactant molecules occurs not on the entire free surface of a solid catalyst, but only on what are called active centers. Thus the general principle of heterogeneous catalyst action consists in that the reactant molecules colliding with the active center of the catalyst can form various unstable intermediates (radical or ions). Both the rate of the reactions and the composition of their products depend on the reactivity and nature of these intermediates. When choosing and employing heterogeneous catalysts, one must take into account of their selectivity, activity, and stability. The stability determines their service life (Erikh, 1988).

2.13 CATALYTIC CRACKING

Catalytic cracking is the process of breaking down larger, heavier and more complex hydrocarbon molecules into simpler and lighter molecules to produce higher value products. It uses heat, pressure and a catalyst. In catalytic cracking, with the aid of the activated clays, pressures of 20 to 40 pounds may be used, with temperatures as low as 900°F In addition, about 50% of the heavy residues which would remain in thermal cracking, will be converted into gasoline with a natural octane rating of 78 to 81, the equivalent of the best motor fuels on today's markets (Erikh, 1988; William D. J. 1979).

Catalytic cracking uses a furnace and reactor. First, crude oil distillation fractions are heated in the furnace and passed to the reactor. In the reactor, the crude meets with a catalyst such as

zeolite. It goes through this step three times, each time getting cooler. Finally, it reaches a step known as separator. The separator collects recycled hydrogen. Then it goes through a fractionator and becomes the final item. Catalytic cracking was introduced to refining in the 30's in response to need for more gasoline and has superseded thermal cracking as it yields more of the desired high octane products. It can virtually double the yield of gasoline type products from a barrel of crude oil. There are two major types of catalytic cracking viz; fixed-bed catalytic cracking, and fluid bed catalytic cracking (Grenall, 1949).

In fixed-bed processes, the catalyst is in the form of small lumps or pellets in layers or beds in several (four or more) catalyst containing drums called converters. Fluid catalytic cracking processes are the most widely used and are characterized by the use of finely powdered catalyst that is moved through the processing unit. The catalyst particles are of such a size that when aerated with air or hydrocarbon vapor, the catalyst behaves like a liquid and can be moved through pipes. Vaporized feedstock and fluidized catalyst flow together into a reaction chamber where the cracking reactions take place (Erikh, 1988).

2.14 ACID ACTIVATION OF CLAY

One of the most common chemical modifications of clays, used for both industrial and scientific purposes, is their acid activation. This consists of the treatment of clay with a mineral acid solution, usually HCl or H_2SO_4. The main task is to obtain partly dissolved material of increased specific surface area, porosity and surface acidity (Komadel, 2003). From the industrial point of view, the term 'acid-activated clays' was reserved mainly for acid-treated bentonites. Bentonite has always had a multitude of markets and acid-activated bentonite was a traditional product for

many decades. It is usually a Ca^{2+} -bentonite that was treated with inorganic acids to replace divalent calcium ions with monovalent hydrogen ions and to leach out ferric, ferrous, aluminium and magnesium ions thus altering the layers of smectite and increasing the specific surface area and porosity. This results in the production of bleaching earths, (Siddiqui, 1968). Other applications of the resulting product include environmentally benign catalysts or their supports, which are used in various chemical reactions such as Friedel-Crafts alkylation, dealkylation and acylation, dimerisation and polymerisation of unsaturated hydrocarbons etc. (Kooli, 1997). It has been discovered that a great similarity exist between the nitrogen-adsorption isotherms of acid-activated montmorillonite clay and those of synthetic silica-alumina gel-type catalysts or of silica gel itself. The similarity is indicative of a common physical structure. It is logical to assume that the siliceous residue left after removal of part of the basic components during the activation treatment is responsible in large part for this similarity (Komadel, 2006).

2.15 CALCINATION OF CLAY

Calcination is the process of subjecting a substance to the action of heat, but without fusion, for the purpose of causing some change in its physical or chemical constitution Greene, 1952). The objects of calcination are usually: (1) to drive off water, present as absorbed moisture, as "water of crystallization," or as "water of constitution"; (2) to drive off carbon dioxide, sulphur dioxide, or other volatile constituent; (3) to oxidize a part or the whole of the substance. There are a few other purposes for which calcination is employed in special cases, but these are the major established reasons. The process of calcinations is often called "roasting," "firing," or "burning," by the workmen. It is carried on in furnaces, retorts, or kilns, and very often the material is raked over or stirred, during the process, to secure uniformity in the product.

The furnaces used for calcining substances vary much in their construction, but there are three general classes: muffle, reverberatory, and shaft furnaces or kilns (Mathers, 1960; Qczuk, 1953).

2.16 BET ADSORPTION ISOTHERM

The BET method is widely used in surface science for the calculation of surface areas of solids by physical adsorption of gas molecules. BET Theory put forward by Brunauer, Emmett and Teller explained that multilayer formation is the true picture of physical adsorption. One of the basic assumptions of Langmuir Adsorption Isotherm was that adsorption is monolayer in nature. Langmuir adsorption equation is applicable under the conditions of low pressure. Under these conditions, gaseous molecules would possess high thermal energy and high escape velocity. As a result of this less number of gaseous molecules would be available near the surface of adsorbent. Under the condition of high pressure and low temperature, thermal energy of gaseous molecules decreases and more and more gaseous molecules would be available per unit surface area. Due to this multilayer adsorption would occur. The multilayer formation was explained by BET Theory. The concept of the theory is an extension of the Langmuir theory, which is a theory for monolayer molecular adsorption, to multilayer adsorption with the following hypotheses: (a) gas molecules physically adsorb on a solid in layers infinitely; (b) there is no interaction between each adsorption layer; and (c) the Langmuir theory can be applied to each layer (Adefila, 2003). The resulting BET equation is expressed by

$$\frac{P/Po}{V(1-P/Po)} = \frac{1}{VmC} + \frac{C-1}{VmC}\left(\frac{P}{Po}\right) \qquad (1)$$

P and P_0 are the equilibrium and the saturation pressure of adsorbates at the temperature of adsorption, v is the adsorbed quantity of the adsorbate and v_m is the monolayer adsorbed gas quantity. c is the BET constant, which is expressed by Equation (2):

$$c = \exp\left(\frac{E_1 - E_L}{RT}\right) \tag{2}$$

E_1 is the heat of adsorption for the first layer, and E_L is that for the second and higher layers and is equal to the heat of liquefaction.

Equation (1) is an adsorption isotherm and can be plotted as a straight line with $(P/P_o) / v[1 - (P/P_o)]$ on the y-axis and P/P_o on the x-axis according to experimental results. This plot is called a BET plot. The linear relationship of this equation is maintained only in the range of $0.05 < P/P_0 < 0.35$. The value of the slope S and the y-intercept I of the line are used to calculate the monolayer adsorbed gas quantity v_m and the BET constant c. The following equations can be used:

Intercept, $I = \frac{1}{VmC}$ and Slope, $S = \frac{C-1}{VmC}$ (3)

Upon mathematical manipulations it follows that: $v_m = \frac{1}{I+S}$ (4)

Employing room temperature and assuming ideal situation, PV = nRT (5)

$$n = \frac{Vm}{M} \tag{6}$$

Hence, $V_{ml} = \frac{VmRT}{MP}$ (7)

Where, R = 8.314 J/(gmol.K)

T = Surrounding temperature (room temperature, 298 K)

M = Molecular mass of the absorbate (18 g/gmole, for water)

V = standard volume at STP (0.0224 m^3)

P = Atmospheric pressure (1.01325×10^5 Nm^{-2})

Area occupied by one volume of adsorbent, α can be derived from the first principle:

Assuming the geometry of the a molecule of the adsorbent is spherical,

Then, Cross sectional area of a molecule, $\alpha = \pi R^2$ **(8)**

Volume of a molecule, $\gamma = \frac{M}{No\rho}$ **(9)**

Where ρ = density of the adsorbate in g/cm^3 (1 g/cm^3).

N_o = Avogadro's constant = 6.023×10^{23} mol^{-1}

Also, $\gamma = 4/3\pi r^3$ **(10)**

Equating Equations (9) and (10), we have: $r = (\frac{3M}{4\pi\rho N_o})^{1/3}$ **(11)**

But r = R, hence, substituting Equation (11) into Equation (8), it follows that;

$$\alpha = 1.209(\frac{M}{\rho N_o})^{2/3} \quad \textbf{(12)}$$

However, the surface area of the adsorbent is calculated as; $S_g = (\frac{Vml\ No}{V})\alpha$ **(13)**

Substituting Equations (7) and (4) into Equation (13), we have $S_g = (\frac{VmRT}{MP} \times \frac{No}{V})\alpha$ **(14)**

Therefore, using Equation (14), S_g can be evaluated in m^2/g (Adefile, 2003).

2.17 X-RAY DIFFRACTION

The X-ray diffraction pattern of a pure substance is like a fingerprint of the substance. About 95% of all solid materials can be described as crystalline while the remaining 5% are amorphous. When X-rays interact with a crystalline substance (Phase), one gets a diffraction pattern. The powder diffraction method is thus ideally suited for characterization and identification of polycrystalline phases. Let us consider the theory behind X-ray diffraction analysis in order to convey an understanding of its fundamental principles (Klung, 1974). In crystalline solids the atoms are arranged in a regular pattern, and there is a smallest volume element that by repetition in three dimensions describes the crystal. This smallest volume element is called a unit cell. The dimensions of the unit cell is described by three axes a, b, c and the angles between them alpha,

beta, gamma. An electron in an alternating electromagnetic field will oscillate with the same frequency as the field. When an X-ray beam hits an atom, the electrons around the atom start to oscillate with the same frequency as the incoming beam. The orientation and interplanar spacings of these planes in the x-ray unit cell of a crystalline material are defined by the three integers h, k, l called indices. A given set of planes with indices h, k , l cut the a-axis of the unit cell in h sections, the b axis in k sections and the c axis in l sections. A zero indicates that the planes are parallel to the corresponding axis. E.g. the 2, 2, 0 planes cut the a– and the b– axes in half, but are parallel to the c– axis. If we use the three dimensional diffraction grating as a mathematical model, the three indices h, k, l become the order of diffraction along the unit cell axes a, b and c respectively. It should now be clear that, depending on what mathematical model we have in mind, we use the terms X-ray reflection and X-ray diffraction as synonyms.

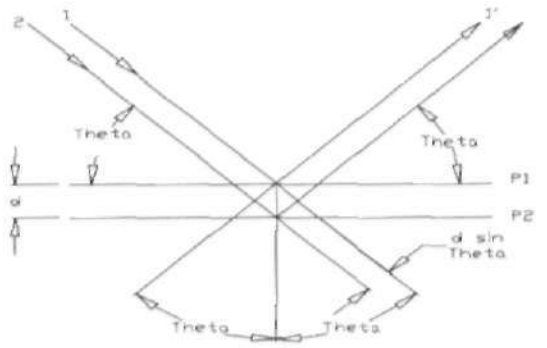


Figure 2.11. Bragg's relation between the incident and diffracted beams (Klung, 1974).

Let us consider an X-ray beam incident on a pair of parallel planes P1 and P2, separated by an interplanar spacing d as shown in Figure 2.11 above. The two parallel incident rays 1 and 2 make an angle (THETA) with these planes. A reflected beam of maximum intensity will result if the waves represented by 1' and 2' are in phase. The difference in path length between 1 to 1' and 2 to 2' must then be an integral number of wavelengths, (LAMBDA).

We can express this relationship mathematically in Bragg's law.

$$2d*\sin\Theta = n * \lambda \qquad (15)$$

The process of reflection is described here in terms of incident and reflected (or diffracted) rays, each making an angle THETA with a fixed crystal plane. Reflections occurs from planes set at angle THETA with respect to the incident beam and generates a reflected beam at an angle 2-THETA from the incident beam. The possible d-spacing defined by the indices h, k, l are determined by the shape of the unit cell. Rewriting Bragg's law we get :

$$\sin\Theta = n\lambda/2d \qquad (16)$$

Therefore, the possible 2-THETA values where we can have reflections are determined by the unit cell dimensions. However, the intensities of the reflections are determined by the distribution of the electrons in the unit cell. The highest electron density are found around atoms. Therefore, the intensities depend on what kind of atoms we have and where in the unit cell they are located. Planes going through areas with high electron density will reflect strongly, planes with low density will give weak intensities (Anonymous[D], 2011).

2.18 X-RAY FLUORESCENCE

X-ray fluorescence (XRF) is the emission of characteristic "secondary" (or fluorescent) X-rays from a material that has been excited by bombarding with high-energy X-rays or gamma rays. It is widely used for elemental analysis and chemical analysis, particularly in the investigation of metals, glass, ceramics and building materials, and for research in geochemistry, forensic science and archaeology (Anonymous[E], 2011).

The underlying physics of XRF entail the ionization of component atoms of materials when they are exposed to short-wavelength X-rays or to gamma rays. Ionization consists of the ejection of one or more

electrons from the atom, and may occur if the atom is exposed to radiation with an energy greater than its ionization potential. X-rays and gamma rays can be energetic enough to expel tightly held electrons from the inner orbitals of the atom. The removal of an electron in this way renders the electronic structure of the atom unstable, and electrons in higher orbitals "fall" into the lower orbital to fill the hole left behind. In falling, energy is released in the form of a photon, the energy of which is equal to the energy difference of the two orbitals involved. Thus, the material emits radiation, which has energy characteristic of the atoms present. The term fluorescence is applied to phenomena in which the absorption of radiation of a specific energy results in the re-emission of radiation of a different energy (generally lower).

Each element has electronic orbitals of characteristic energy. Following removal of an inner electron by an energetic photon provided by a primary radiation source, an electron from an outer shell drops into its place. The main transitions are given names: an L→K transition is traditionally called Kα, an M→K transition is called Kβ, an M→L transition is called Lα, and so on. Each of these transitions yields a fluorescent photon with a characteristic energy equal to the difference in energy of the initial and final orbital. The wavelength of this fluorescent radiation can be calculated from Planck's Law:

$$\lambda = h \cdot c / E \tag{17}$$

The fluorescent radiation can be analysed either by sorting the energies of the photons (energy-dispersive analysis) or by separating the wavelengths of the radiation (wavelength-dispersive analysis). Once sorted, the intensity of each characteristic radiation is directly related to the amount of each element in the material. This is the basis of a powerful technique in analytical chemistry.

In order to excite the atoms, a source of radiation is required, with sufficient energy to expel tightly held inner electrons. When the energy source is a synchrotron or the X-rays are focused by an optic like a polycapillary, the X-ray beam can be very small and very intense. As a result, atomic information on the sub-micrometre scale can be obtained. X-ray generators in the range 20–60 kV are used, which allow excitation of a broad range of atoms. The continuous spectrum consists of "bremsstrahlung" radiation: radiation produced when high-energy electrons passing through the tube are progressively decelerated by the material of the tube anode (the "target").

Energy dispersive analysis of a sample can be carried out using the XRF; the fluorescent X-rays emitted by the material sample are directed into a solid-state detector which produces a "continuous" distribution of pulses, the voltages of which are proportional to the incoming photon energies. This signal is processed by a multichannel analyser (MCA) which produces an accumulating digital spectrum that can be processed to obtain analytical data. In wavelength dispersive analysis, the fluorescent X-rays emitted by the material sample are directed into a diffraction grating monochromator. The diffraction grating used is usually a single crystal. By varying the angle of incidence and take-off on the crystal, a single X-ray wavelength can be selected. The wavelength obtained is given by the Bragg Equation:

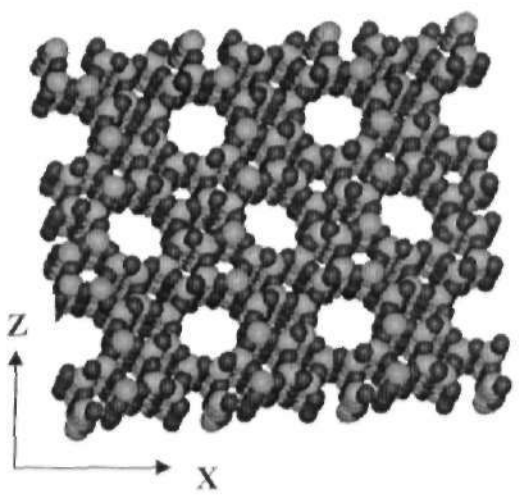
$$n \cdot \lambda = 2d \cdot \sin(\theta) \tag{18}$$

where d is the spacing of atomic layers parallel to the crystal surface.

Chemical analysis of a sample is carried out by employing a primary X-ray beam to excite fluorescent radiation from the sample (Anonymous[E], 2011).

2.19 ZEOLITE CATALYST

Compositionally, zeolites catalysts are similar to clay minerals. More specifically, both are alumino-silicates. They differ, however, in their crystalline structure. Many clays have a layered crystalline structure (similar to a deck of cards) and are subject to shrinking and swelling as water is absorbed and removed between the layers. In contrast, zeolites have a rigid, 3-dimensional crystalline structure (similar to a honeycomb) consisting of a network of interconnected tunnels and cages of narrow pores giving very high internal surface area. Water moves freely in and out of these pores but the zeolite framework remains rigid. Another special aspect of this structure is that the pore and channel sizes are nearly uniform, allowing the crystal to act as a molecular sieve. The porous zeolite is host to water molecules and ions of potassium and calcium, as well as a variety of other positively charged ions, but only those of appropriate molecular size to fit into the pores are admitted creating the selectivity property of zeolite. When used in catalyst fabrication, zeolite represents the active phase which is impregnated on a support matrix which can be mainly clay to enable fabrication of shaped products to adjust the mechanical properties of the adsorbent (Sherman, 1999).



RECEIVED
16 MAY 2012
ABMADU BELLO UNIVERSITY
ZARIA

Figure 2.12: Pictorial illustration of zeolite crystal structure (http://en.wikipedia.org/wiki/x_ray crystallography/15/12/2011).

489481

CHAPTER 3

MATERIAL, EQUIPMENT AND METHODOLOGY

Details of the research procedures employed are discussed in this chapter. The materials and equipment used are first listed.

3.1 MATERIALS AND EQUIPMENT

Different types of material and equipments were used to carry out the experimental work of this research, they are listed as follows:

3.1.1 List of Materials

1. 98% Conc. Sulfuric acid.
2. Tap water.
3. Raw Pindiga Bentonite clay.
4. Distilled water.
5. Magnesium chloride.
6. Potassium sulphate.
7. Calcium sulphate.
8. Sodium acetate.

3.1.2 List of Apparatus

1. Membrane filter with pore size 0.2 μm.
2. Spatula.
3. Beakers (100-500ml)
4. Measuring cylinders (50 - 250ml)
5. Tyler sieve (Mesh size 230)
6. Glass funnel
7. Plastic buckets
8. Clay pots
9. Ceramic crucible (25ml – 75ml)
10. Air tight desiccators
11. Ceramic mortar and pestle
12. Wooden mortar and pestle.

3.1.3 List of Equipment

1. Electric furnace. (Nabertherm; 30 - 1400°C)
3. Electric oven (NYC – 101; 30 - 400°C, Nabertherm; 30 - 650°C)
4. Weighing balances (Weda, T18; 0 – 100kg, Metler Toledo; AB204; 0 - 210g)
5. Stop watch
6. X-ray diffraction (Stchmabzu, 6000).
7. X-ray fluorescence (Pananalytical, Minipal 4).
8. Electric stirrer (Trieb, 73 – 660 rpm)

3.2 EXPERIMENTAL PROCEDURE

The experimental procedures are as follow:

3.2.1 Raw Materials Collection

Raw Pindiga bentonitic clay was collected form the Center for Energy Research and Training, Ahmadu Bello University, Zaria. The raw clay sample was said to be mined from Pindiga formation at Pindiga Local Government Area in Gombe state by representative mining.

3.2.2 Beneficiation

The raw clay was wet-beneficiated in order to purify it from physically and chemically combined impurities such as metallic oxide, soluble salts and grits such as; Fe_2O_3, FeO, MgO, CaO, MnO, Na_2O, K_2O, $MgSO_4$, $CaSO_4$, Na_2SO_4, K_2SO_4, Na_2CO_3, K_2CO_3, $MgCO_3$, $CaCO_3$, etc. The raw clay was crushed and ground using wooden mortar and pestle. Then, the ground clay was wet-beneficiated using an experimentally determined optimum mixing ratio of 0.1kg:1lt of clay to water, and optimum settling time of 24 hrs. After allowing the clay to soak properly for 24 hrs the mixture was blunged by vigorously stirring at 400 rpm for 3hours so as to separate all the agglomerates of clay particles. Then the mixture was further allowed to settle overnight. The next day the blunged clay slurry settled into three clear layers; the bottom coarse particles; the middle fine clay particles and the top supernatant water layer. The three layers were separated by siphoning. The top supernatant water layer and the bottom coarse particles were discarded and the middle fine clay slurry layer was further processed. The fine clay slurry was sieved using Tyler sieve of mesh size 230 (63μm aperture opening) so as to further separate the fine grits present in the fraction. The resulting clay slurry was allowed to settle and the supernatant water

layer was separated by siphoning in intervals of 2 hours, until there was no reasonable quantity of supernatant water layer. Then the fairly thick slurry was poured into an open clay-pot to ensure faster separation of the water through the micro-pores of the clay-pot surface. At the same time the top supernatant water layer was siphoned in intervals of 4hrs for 6days. A relatively thick slurry was observed after 6days, but when subjected to hydraulic press a lot of the clay particles escaped with the water. Therefore, the slurry was returned to the clay-pot for open drying at room temperature. Therefore, was completely dried to solid bentonite cake after another 2days. Then Finally the solid clay cake was dried in an electric oven at 300°C for 3hours.

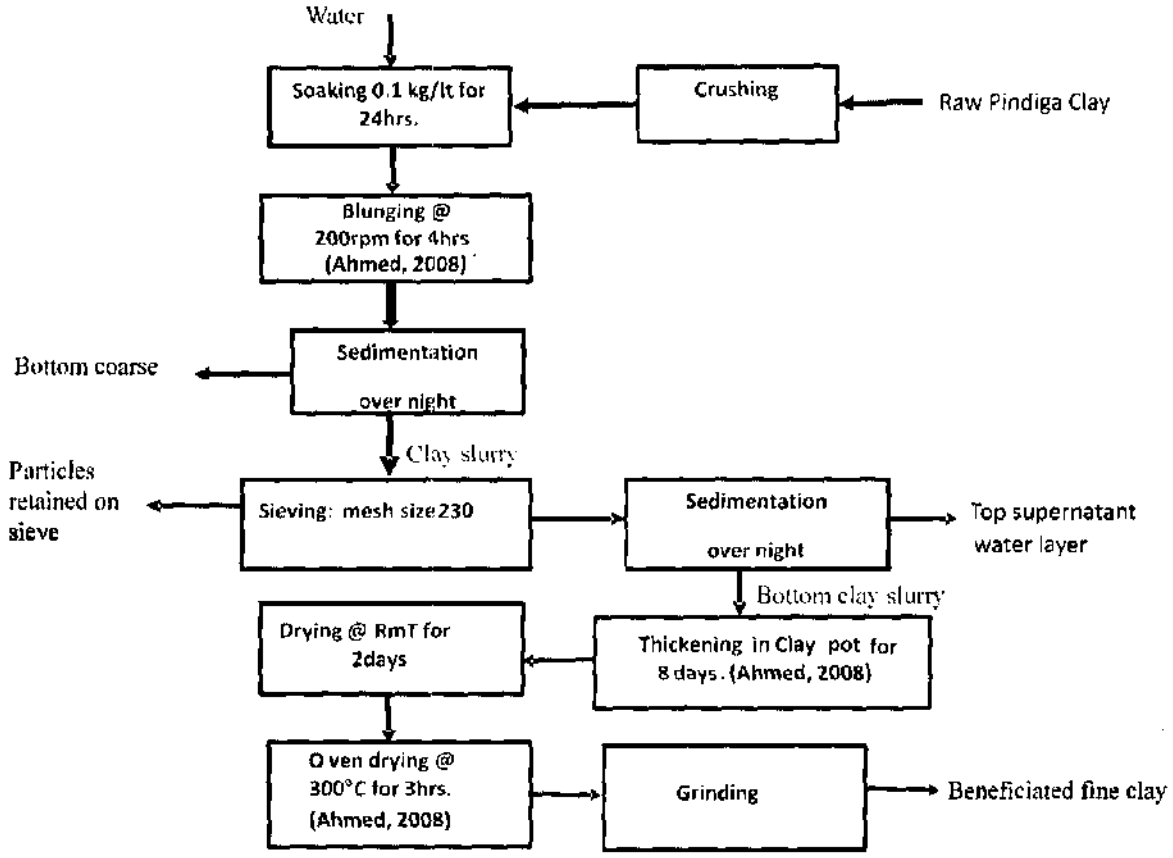


Figure 3.1: Flow diagram of the raw clay beneficiation process

3.2.3 Clay Calcination

The beneficiated clay was ground to powder form, then oven-dried at 300°C for 3hrs to constant weight, the clay samples were then calcined at varying temperatures of 700°C, 750°C and 800°C for constant time of 3 hours.

3.2.4 Clay Acidification

The calcined clay was activated by acidification using sulfuric acid. Two types of acidification processes were employed; wet and dry acidification.

Dry Acidification: The calcined clay was sieved using using Tyler sieve of mesh size 230 (63µm aperture opening) and then concentrated sulfuric acid was sprayed over the clay powder in an acid-to-clay ratio of 0.3:1 at at room temperature with vigorous stirring. Then the resulting moist clay was open dried at room temperature.

Wet Acidification: The calcined clay was sieved using using Tyler sieve of mesh size 230 (63µm aperture opening) then 30g of the clay powder was soaked in 120ml of 6M sulfuric acid at 95°C for 8hours. After the reaction the mixture was filtered using 0.2 µm filter paper. The liquid filtrate was disposed and the wet clay residue was washed with distilled water then open dried at room temperature.

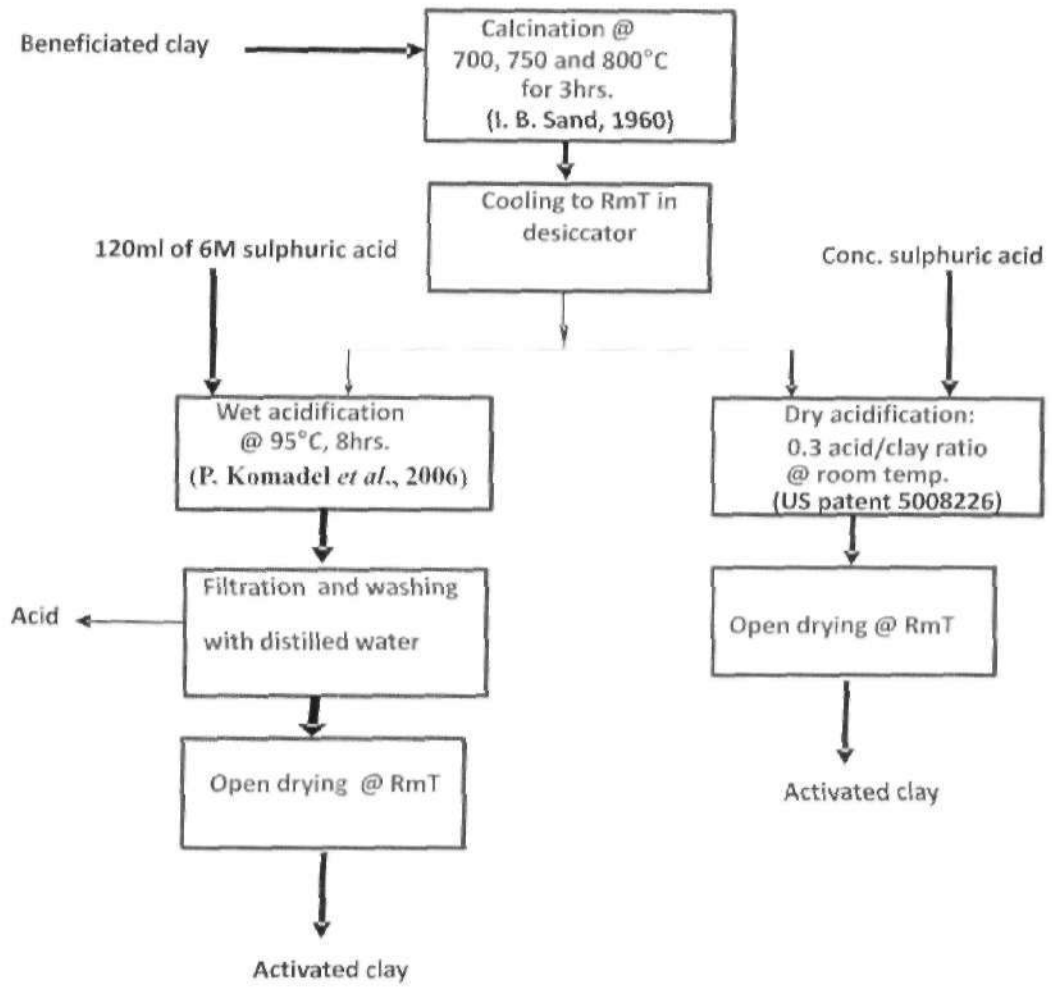


Figure 3.2: Flow diagram of the clay calcination and acidification processes

3.2.5 Determination of Surface Area

The surface area was determined using an adopted BET method developed by Adefila et al (2003) which employs adsorption of adsorbate, water molecules on the surface of the adsorbent samples using the BET theory. In this method an adsorbate constant relative humidity was established as the saturated vapour pressure of a saturated salt solution. Therefore, a saturated salt solution was prepared and kept in an air tight desiccator with a 1.0 g quantity of the adsorbent evenly spread on a Petri dish and kept together with the saturated salt solution in the air tight desiccators for 24 hrs maintaining the laboratory temperature at room temperature. The

weight gain of the sample determined at the end of the 24 hrs was used to represent V in Equation (1), above (Section 2.15), and the constant relative humidity of the adsorbate was used to represent P/P_o of the same equation. Also, three samples of known BET surface area values were used as standards to establish the correction factor of the method.

Relative Humidity of Adsorbate: The constant relative humidity of the adsorbate used in the experiment was determined by preparing two saturated solutions of a particular salt, one was kept in an air tight desiccator and the other left open in the laboratory, the two were left for 24hrs., noting their respective weight at the beginning and at the end of 24hrs. The relative humidity of the saturated salt solution was evaluated as the ratio of the weight differences of salt solution in desiccator (at initial point and after 24hrs) to the weight differences of salt solution left open (at initial point and after 24hrs) (Adefila *et al*, 2003).

3.2.6 Characterization of Clay Samples

The raw, beneficiated, calcined and acidified samples were characterized to determine their physical, chemical and mineralogical properties.

3.2.6.1 Physical properties

The specific densities of the raw and beneficiated clay samples were determined using the laboratory density bottle method, their pH values were determined using a pH meter and their specific surface areas were determined as discussed above.

3.2.6.2 Chemical composition

Chemical composition of each sample was determined using a Minipal 4, Pananalytical X-ray fluorescence, analyzer, at Nigerian Geological Survey Agency, Kaduna.

3.2.6.3 Mineralogical Composition

The crystal phases present in the samples were determined using a Stchmabzu, X-ray diffractometer, model 6000, at National Steel Raw Materials Exploration Agency, Kaduna. The patterns were recorded from Bragg's angle of 0° to 40°, at a sampling pitch of 0.020°, scanning speed of 4.00 deg/min, preset time of 0.30 min. using CuKα target X-ray radiation.

CHAPTER 4

RESULTS AND DISCUSSION

This chapter presents all the results generated from the investigations and their discussion

4.1 DETERMINATION OF PHYSICAL PROPERTIES

Table 4.1 shows the results of the specific density and the pH determinations. Detail evaluation of data is presented in Appendix A.

Table 4.1: Results of density and the pH measurements for the Pindiga bentonitic clay

SAMPLE	SPECIFIC DENSITY	pH VALUE
RAW CLAY	2.58	7.9
BENEFICIATED CLAY	2.45	6.5
CAL. 700 °C	2.45	6.3
CAL. 750 °C	2.48	6.2
CAL. 800 °C	2.55	5.9
ACF (WET) 700 °C	2.27	2.3
ACF (WET) 800 °C	2.33	2.4
ACF (DRY) 700 °C	2.26	2.8
ACF (DRY) 800 °C	2.25	2.8

It was observed that the raw Pindiga clay which had specific density of 2.58 became less dense on beneficiation to a specific density value of 2.45. This was likely due to removal of some dense impurities suspected to be predominantly quartz (specific density of quartz is 2.66). On calcination to 700 °C the specific density remained at 2.45. However, after calcination to 750 °C

and 800 °C the specific density increased to 2.48 and 2.55 respectively. This was likely due to removal of the physically combined water which was more pronouncedly removed at the higher calcination temperatures. The wet acidified samples were less dense with specific density values of 2.27 to 2.33. This was likely due to the acid leaching of the alumina which is the denser component of the clay structure, leaving the less dense silica. Nevertheless, the dry acidified samples also had low specific density values of 2.25 to 2.26, this was likely due to the formation of sulphate salt which is less dense than clay.

It was also observed that the pH value of the raw Pindiga clay reduced from 7.9 to 6.5 after beneficiation, making the slightly basic raw clay to become slightly acidic. This may be due to removal of basic impurities such as soluble salts. After calcination the pH values reduced further to 6.3, 6.2 and 5.9 for cacination temperature of 700 °C, 750 °C and 800 °C respectively. This may be due to the effect of decomposition of some basic impurities such as sodium carbonate salt. However, the low pH values obtained for the acidified samples were understandably due to the effect of the acid; they have become more.

4.2 DETERMINATION OF SURFACE AREA

Using the BET isotherm Equations (1) – (14) as discussed in Chapter 2, Section 2.16, the relative humidity (P_o/P) of the adsorbate was calculated from the relative humidity of the saturated salt solution as discussed in Chapter 4. Detailed experimental data and their evaluations are presented in Appendix B. The summary results for the BET surface area are presented in Tables 4.2 and 4.3.

Table 4.2: Measured BET surface area of standard samples used to determine correction factor for the test method.

STANDARD	ACTUAL SURFACE AREA (m^2/g)	SURFACE AREA OBTAINED (m^2/g)	ERROR (%)
A	166.16	198.84	19.67
B	155.20	185.85	19.75
C	3.00	3.60	20.06
Average error = + 19.8267%			
Correction factor = 1 – 0.198267 = 0.8017			

Table 4.3: Measured BET surface area of the clay samples

SAMPLE	SLOPE, S (g^{-1})	V_M (g)	S_g (m^2/g)	CORRECTED S_g (m^2/g)
RAW	134.20	0.00745	32.87	26.35
BENEFICIATED	79.74	0.01254	54.65	43.81
CAL. 700°C	36.50	0.02741	121.39	97.31
CAL. 750°C	32.54	0.02814	123.89	99.32
CAL. 800°C	25.28	0.03956	174.12	139.59
ACF (WET) 700°C	18.74	0.05336	238.76	191.41
ACF (WET) 800°C	13.20	0.07576	337.33	270.44
ACF (DRY) 700°C	9.81	0.10194	454.94	364.73
ACF (DRY) 800°C	8.81	0.11352	504.53	404.48

The raw clay had a low surface area of 26.35 m^2/g which was far below the literature range of 150 – 350 m^2/g (Bourane, 2011). After beneficiation 66% improvement was noted and up to 269% improvement was observed after calcination at 700°C with further increment at 750°C and 800°C. However, much more substantial increment was experienced after acidification.

Even though the surface area results obtained after dry acidification (364.73 and 404.48 m^2/g) were larger than after wet acidification (191.41 and 270.44 m^2/g), this is likely because of the presence of the sulphate salts (which are hygroscopic) produced during the dry acidification process, whereas, the wet acidification samples were free of such sulphate salts because the sulphate salts produced during the wet acidification process may have been washed away with distilled water.

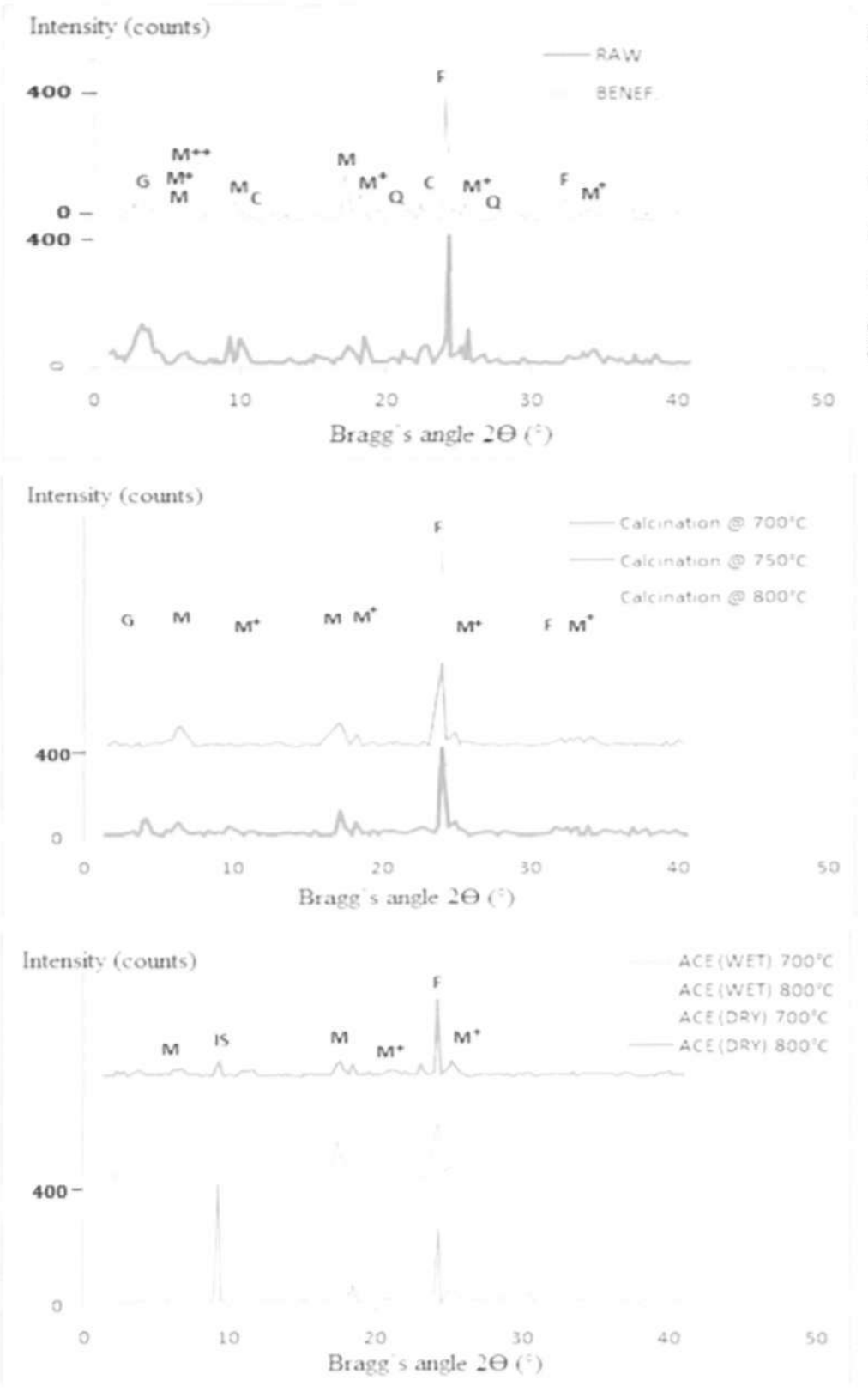
The BET method used gave average error of +19.8267% of the actual BET surface area values expected due to some inherent error introducing factors associated with the method, such as; ideal situation assumption, efficiency of the desiccator used, purity of the salts used, etc.

4.3 MINERAL COMPOSITION

The crystal phases present in the samples were determined by XRD analysis. Results of the XRD patterns obtained are presented in Figure 4.1. From the result it can be observed that the consistency of the Ca-montmorillonite peaks was an indication that the clay mineral was mainly Ca based bentonite. However, the prominent peak of iron oxide indicated that the clay contained reasonable iron (Fe) impurity.

The beneficiation was effective as reflected in the beneficiated sample's XRD leading to reduction in the XRD peaks for quartz and organic impurities (in the form of carbon (C) and graphite (G)).

Looking at the XRD pattern for the raw clay, it can be observed that a blurred prominent peak of organic impurity (G), and some soluble salts occurred at around $2\Theta = 3°$. However, the peak became clearer and suppressed after beneficiation, indicating reduction of organic impurities, quartz and soluble salts.



M: Ca-montmorillonite

M^{+}: K-montmorillonite

M^{++}: Na-montmorillonite

M^{+++}:

Mg-montmorillonite

F: Ferric oxide

C/G/Q: Carbon/graphite/quartz

Figure 4.1. XRD patterns for the various samples of Pindiga clay

4.4 CHEMICAL COMPOSITION

Table 4.4 presents the summary of the XRF results obtained. As already observed from the XRD results, the XRF results further confirmed the presence of iron impurity; with concentration as high as 26.54 wt% in the raw clay. Traces of other heavy metals such as Vanadium, Nickel, Copper, Titanium, Manganese Barium, Ytterbium, etc. can also be detected by the XRF as shown in the results presented in Table 4.4 for the raw clay.

Table 4.4: Chemical composition of the raw, beneficiated and treated Pindiga clay

COMPONENT (%)	RAW	BENF.	Calcined (700 °C)	Calcined (750 °C)	Calcined (800 °C)	ACF800 (DRY)	ACF700 (DRY)	ACF700 (WET)	ACF800 (WET)
Al_2O_3	14.00	15.00	18.00	17.10	16.90	13.00	11.00	11.00	10.00
SiO_2	43.60	45.90	51.70	49.50	48.60	33.80	39.80	52.40	52.80
K_2O	1.32	1.09	0.97	0.84	0.94	0.75	0.67	0.43	0.45
CaO	2.46	2.00	1.76	1.83	1.90	1.61	2.40	1.55	1.73
Na_2O	1.00	1.19	0.99	1.27	1.24	0.88	1.02	0.81	0.86
MgO	0.05	0.10	0.32	0.28	0.16	0.29	0.36	0.19	0.24
TiO_2	2.06	2.15	1.88	1.98	2.03	1.52	2.20	2.29	2.27
V_2O_5	0.10	0.10	0.12	0.12	0.10	0.081	0.12	0.11	0.12
Cr_2O_3	0.051	0.049	0.042	0.041	0.047	0.031	0.042	0.033	0.037
MnO	0.38	0.18	0.15	0.17	0.17	0.14	0.16	0.073	0.075
Fe_2O_3	26.54	24.15	19.79	22.15	22.28	18.30	21.60	15.34	12.80
NiO	0.01	0.02	0.01	0.02	0.02	-	-	0.02	0.01
CuO	0.049	0.037	0.031	0.038	0.030	0.031	-	0.027	0.028
ZnO	0.070	0.075	0.055	0.073	0.061	0.066	0.062	0.01	0.02
BaO	0.24	0.24	-	-	0.22	0.16	-	-	-
Eu_2O_3	0.31	0.25	0.26	0.25	0.22	0.20	0.25	0.17	0.18
Yb_2O_3	0.03	0.02	-	-	0.01	-	-	0.02	0.02
Re_2O_7	0.10	0.10	0.10	0.10	0.10	0.10	0.20	0.10	0.18
SO_3	1.00	-	-	-	0.085	23.20	15.73	11.73	12.63
MoO_3	-	-	-	-	-	2.3	0.20	-	0.50
L.O.I	6.46	6.63	3.67	4.21	4.53	2.83	3.62	3.09	4.24
TOTAL	99.83	99.28	99.85	99.97	99.64	99.29	99.43	99.39	99.19

The iron impurity in the raw clay was mostly in the form of Ferric oxide (Fe_2O_3), which was slightly soluble (2.39%) as can be observed from the reduction of Fe_2O_3 from 26.54% for the raw clay, to 24.15% after beneficiation, as shown in the XRF results.

From the XRF results, the reduction in the percentages of K_2O, Na_2O and CaO and the disappearance of SO_3 from the raw clay to the beneficiated clay further indicated that soluble salts of these metals in sulphate forms were dissolved away during beneficiation. After the calcination processes the XRF results showed increase in the alumina and silica content of the clay. This was due to decomposition of some organic impurities and salts.

Even though the percentages of K_2O, Na_2O and CaO decreased from raw to beneficiated, and down to calcined-clay as already discussed, the reduction in the percentage of CaO was relatively lower, indicating that the clay mineral was majorly Ca based bentonite.

However, the insoluble Fe_2O_3 left after beneficiation remained as the dominant impurity even after calcination and dry acidification, however, it was reduced after the wet acidification processes as can be observed from the XRF results.

From the XRF it can be observed that both the two wet acidification processes resulted in higher reduction in Fe_2O_3. However, the reduction when the sample calcined at 700°C was used was slightly more than when sample calcined at 800°C was used (12.80% and 15.34% respectively). Furthermore, it was observed that another XRD peak resulted at around $2\Theta = 9°$ after wet

acidification of sample calcined at 700°C which was suspected to be insoluble iron sulphur compound produced as result of the attack of the sulphuric acid on the Fe_2O_3.

Apart from the iron impurity, a little pronounced quantity of other heavy metals impurities such as titanium, vanadium, and manganese were observed in optimum sample up to the amount of 2.27, 0.12 and 0.075 respectively. These quantities may have effect on the catalytic activities of a catalyst if this material is used as a catalyst support.

In the XRF results, only 1% SO_3 was observed in the raw clay, which became 0% after beneficiation as well as after calcinations. However, this rose to 14 and 24% during dry acidification and to 10 and 13% during wet acidification for the samples calcined at 700°C and 800°C respectively. On the other hand, the alumina content, which was 14% in the raw clay reduced during these acidification stages up to 10% while silica increased from 43% in the raw clay to 52% in the wet acidified clay. Therefore, these indicated that the sulphuric acid added during the acidification had leached out some alumina in the form of aluminum sulphate, making the clay more siliceous.

CHAPTER 5

CONCLUSIONS AND RECOMMENDATIONS

5.1 CONCLUSIONS

The following conclusions may be made from the investigations carried out.

1. The Pindiga clay investigated in this work was mainly Ca-base bentonitic clay which contains some Na, K, and Mg-base Bentonites, as shown by the XRD patterns of the clay.

2. The BET surface area of the raw clay was very low, hence, the raw clay was not suitable for application as a catalyst support. However, upon calcination and activation by acid treatment, the surface area of the clay improved immensely and the clay is expected to be suitable for use as zeolite catalyst support. The raw clay contained very high level of ferric oxide impurity up to 26.54 wt%, with only slight reductions at the various stages of treatment. Nevertheless, the best reduction was obtained after wet acidification of 800°C calcined sample bringing the iron impurity to 12.80 wt%. Meaning that if 60% of the material is used in catalyst formulation, there will be up to 7.68% iron impurity which is still high when compared to the literature requirement of less than 1 wt% (Yuxia, 2007).

3. Similarly if 60% of the material is used in catalyst formulation, the quantities of titanium, vanadium, and manganese impurities that will be present will be 1.36, 0.07 and 0.04 wt% respectively. Hence, in the case of titanium, this quantity will have effect on the catalytic activities of the catalyst since its above the literature requirement of less than 1 wt% (Yuxia, 2007). Nevertheless, the quantity of vanadium, and manganese (including other

heavy metals in this range) that will be present in the catalyst will have no significant impact on the activity of the catalyst.

4. Even though the surface area results obtained after dry acidification were larger than after wet acidification, the surface area of 270.44 m^2/g obtained after wet acidification of 800°C – calcined sample can be taken to be the optimum surface area value due to the fact that unlike the dry acidification method samples, the wet method samples produced had minimum hygroscopic sulphate salts which will interfere with the surface area result. Moreover, this value conformed with the established surface area requirement of montmorillonite clay support (150 – 350 m^2/g, (Bourane, 2011)) for FCC catalyst.

5. From the foregoing, it can be concluded that wet acidification of 800°C calcined Pindiga clay with mixing ratio of 30g of the clay powder in 120 ml of 6M sulfuric acid at 95°C for 8 hours is expected to produced a good material from Pindiga clay which can be used as a potential support material for catalyst if the iron content can be reduced significantly.

5.2 RECOMMENDATIONS

From the foregoing the following recommendations can be made.

1. Further work should be carried out to remove high iron impurity of Pindiga bentonitic clay and the level of the vanadium impurity should also be reduced further.

2. Further work should be carried out on the DTA or DSC analysis of the treated samples to determine their thermal behaviour.

3. Further work should be carried out on the selected treated clay samples for zeolite catalyst support to determine their performance and thermal stability.

4. Further work should be carried out on other bentonitic clays in the country with lower iron impurity.

REFERENCE

Abdennour, B., Refa, K. O., Salem, A. M., Dean, C. F,, AbdulBari, S. M., Shakeel, A. (2011). Metallic Clay Based FCC Gasoline Sulphur Reduction Additive Compositions. United States patent No. 20110120912.

Adefila, S.S. Aderemi, B.O., Ajayi, O.A. and Baderin, D.A. (2003). Comparative Surface Area Determination Using Water Adsorption Method: *Nigerian Journal of Engineering* 11, (2) 88-95.

Aderemi, B.O and Ajayi O.A. (2002). Sourcing Aluminum from Kaolin Clay for Metallurgical Industry: Conference Proceedings of the First Nigerian Materials Congress, Held at Engineering Materials Development Centre, Akure, November. P 104- 107.

Ahmed, A. S. (2008). Properties of Kaolin and Methods of Beneficiation: Proceedings of the First Nigerian Conference on Zeolite, Organized by PTDF Professorial Chair in Chemical Engineering, Ahmadu Bello University, Zaria, Held at Institute of Development Research, ABU., Zaria, P. 1 – 17.

Anonymous[(A)]: http://en.wikipedia.org/wiki/Clay: Clay Mineral Wikipedia, Retrieved on 08/10/2011

Anonymous[(B)]: aquatechnologies.com: Manufacturers Direct Water Treatment Technologies, Retrieved on 20/11/2011

Anonymous[(C)]: http://en.wikipedia.org/wiki/Bentonite: Bentonite Mineral Wikipedia, Retrieved on 08/10/2011

Anonymous[(D)]: en.wikipedia.org/wiki/x_raycrystallography: X-ray Crystallography Wikipedia, Retrieved on 08/10/2011

Anonymous[(E)]: en.wikipedia.org/wiki/x_rayflourescence: X-ray Flourescence Wikipedia, Retrieved on 15/12/2011

Erikh, V. N., Rasina, M. G. and Rudin, M. G. (1988). "The Chemistry and Technology of Petroleum and Gas" Mir Publisher, Moscow.

Ferris, J. (2000). Clay-Catalyzed RNA Polymerization Activity An Overview Center for study on the origin of life, New York, USA

George, L. B. Jr., and Lafayette, G. K. (2008). A Study of Specific Surface Area for Matrix, EheimSubstrat Pro, and JBL MicroMec; Seachem Laboratories.

Greene-Kelley, R. (1952). Irrevcrsible Dehydration of Montmorillonite: *Clay Mineral. Bulletin*, 1, 221-227.

Grenall, A. (1949). Montmorillonite Cracking Catalyst*: Indus. Eng. Chem.*, 4, 1485-1489.

Interrante, L. V. and Hampden-Smith, M. J. (1998). "Chemistry of Advanced Materials" University of New Mexico USA., John Wiley & Sons USA.

Klung, H. P. (1974). "X-ray Diffraction Procedure for Polycrystalline and Amorphous Materials". John Wiley & Sons, Inc. New York.

Komadel, P. and Madejova, J. (2006). Acid Activation of Clay Minerals: *Handbook of Clay Science. Elsevier Ltd.* 1, 263-274

Komadel, .P and Madejova, J. (1997). Acidity And Catalytic Activity of Mildly Acid-Treated Mg-Rich Montmorillonite and Hectorite: *Journal of the Chemical Society*, 93 4207–4210.

Kooli, F. and Jones, W. (1997). Characterization and Catalytic Properties of a Saponite Clay Modified by Acid Activation: *Clay Minerals, Journal of Fine Particle Science*, 32 633-643

Mathers, A. C., Weed, S. B. and Coleman, N. T. (1960). "The Effect of Acid and Heat Treatment on Montmorillonoids." North Carolina State College.

Meor, Y. M. S., Muslimin, M. (2007). Synthesis of Alumina Using the Solvothermal Method: *The Malaysian Journal of Analytical Science*, 11, (1) 262-268.

Qczuk, B. A., Chibowski, E., Hajnos, T. M., Biaeopiotrowicz, T., Earley, J. W., Osthaus, B. B., and Milne, I. H. (1953). Purification and Properties of Montmorillonite: *Am. Mineral.*, 38, 707-724.

Sand, L. B and Crowley, M. S. (1960). Comparison of a Natural Bentonite with its Synthetic Analogue: Report Note, University of Utah, Salt Lake City, Utah, and the Pennsylvania State University, University Park, Pennsylvania.

Sherman, J.D. (1999), Synthetic Zeolites and Other Microporous Oxide Molecular Sieves: *Proceedings of the National Academy of Sciences*, 96, (7) 3471-3478.

Siddiqui, H. M. K. (1968). "Bleaching Earths" Pergamon Press Muze Inc. USA

Trimm, D. L. (1980). "Design of Industrial Catalysts". Elsevier Scientific Publishing Company, New-York. P 91–187.

William D. J. (1979). Clay Minerals Catalysis and Petroleum Generation: *Annual Review of Earth and Planetary Sciences*.7, 183-198

Wilson J. W. (1997). "Fluid Catalytic Cracking Technology and Operations", Pennwell publishing company. John Wiley & Sons, Inc. New York.

489481

Woertink, J. S., Smeets, P. J., Groothaert, M. H., Vance, M. A., Sels, B. F., Schoonheydt, R. A. and Solomon, E. I. (2009). A $[Cu_2O]^{2+}$ Core in Cu-ZSM-5, the Active Site in the Oxidation of Methane to Methanol: *Proc. Natl. Acad. Sci. U S A.*, 10; 106, (45) 18908–18913.

Wojciechowska, R. Wojciechowski, Kaminski, W. J., (1988). Thermal Decomposition of Ammonium and Potassium Alums: *Journal of Thermal Analysis*, 33 503-509.

Xie, Z, Liu, Z., Wang. Y., Yang, Q., Xu, L., and Ding, W. (2010). An Overview of Recent Development in Composite Catalysts from Porous Materials for Various Reactions and Processes: *Int J Mol. Sci.* 11, (5) 2152–2187.

Xin, Y. (2011). "Process for Making Acid Activated Bleaching Earth Using High Susceptibility Source Clay and Novel Bleaching Earth Product". XinyuanTechnology Co., Ltd

Yuxia, Z., Quansheng, D., Wei, L., Wei, T., Liwen, T. and Jun, L. (2007). Study of Iron Effect on FCC Catalysts. *Method and process innovations Elsevier B.V.*

APPENDIX A

Evaluation of Specific Density Results

Table A. Results of the specific density determination for the raw and beneficiated clay samples.

SAMPLE	W_1 (g)	W_2 (g)	W_3 (g)	W_4 (g)
Raw	23.0975	42.2958	84.8830	73.1392
Beneficiated	23.0975	45.3352	86.2926	73.1392
CAL. 700 °C	19.9507	38.1853	80.841	70.0412
CAL. 750 °C	19.9507	34.4768	78.7114	70.0412
CAL. 800 °C	19.9507	37.7992	80.8923	70.0412
ACF (WET) 700 °C	19.9507	30.332	75.857	70.0412
ACF (WET) 800 °C	19.9507	27.6505	74.4354	70.0412
ACF (DRY) 700 °C	19.9507	28.2653	74.6715	70.0412

W_1 = weight of empty bottle

W_2 = weight of bottle + clay

W_3 = weight of bottle + clay + water

W_4 = weight of bottle + full water

$$\text{Specific density of clay, } G = \frac{W2 - W1}{(W4 - W1) - (W3 - W2)} \qquad (A1)$$

Therefore; $G_{raw} = \frac{42.2958 - 23.0975}{(73.1392 - 23.0975) - (84.8830 - 42.2958)} = 2.58$

Therefore; $G_{benf} = \frac{45.3352 - 23.0975}{(73.1392 - 23.0975) - (86.2926 - 45.3352)} = 2.45$

APPENDIX B

Evaluation of BET Surface Area Results

Equation (12) can be simplified as:

$$\alpha = 1.209\left(\frac{M}{\rho N_o}\right)^{2/3} = 1.209 \times \left(\frac{18\frac{g}{gmol}}{1\frac{g}{cm3} \times 6.023E23\frac{1}{mol}}\right)^{2/3} = 1.1643 \times 10^{-15}\ cm^2$$

$$= 1.1643 \times 10^{-19}\ m^2$$

Therefore, Equation (14) can be simplified as:

$$S_g = \left(\frac{VmRT}{MP} \times \frac{No}{V}\right)\alpha = V_m\left(\frac{RT}{MP} \times \frac{No}{V}\right)\alpha$$

$$= V_m\left(\frac{8.314\frac{J}{gmol.K} \times 301K \times 6.023E23\frac{1}{mol}}{18\frac{g}{gmol} \times 1.01325E5\frac{N}{m2} \times 0.0224\ m3}\right) \times 1.1643 \times 10^{-19}\ m^2 = (4295.534\ m^2/g) \times V_m$$

Note, V_m = Monolayer adsorbed water molecule quantity (in g) per unit g of the adsorbent.

Table B1. Data for determination of relative humidity of saturated salt solutions

SALT	Q_{D1}	Q_{D2}	Q_{O1}	Q_{O2}	RH
$CaSO_4$	39.9701	39.8034	40.04	35.2753	0.0350
K_2SO_4	50.2288	49.8943	47.85	42.7947	0.0661
CH_3COONa	59.4566	59.1621	63.08	61.8193	0.2338
$MgCl_2$	41.6825	41.3087	42.08	40.7292	0.2763

Where $RH = \frac{QD2 - QD1}{(QO2 - QO1)} = (P/P_o)$ (B1)

Where, Q_{DI} = Initial weight of salt solution in desicator.

Q_{DI} = final weight of salt solution after 24hrs. in desicator.

Q_{OI} = Initial weight of salt solution open to room condition.

Q_{O2} =final weight of salt solution open to room condition for 24hrs.

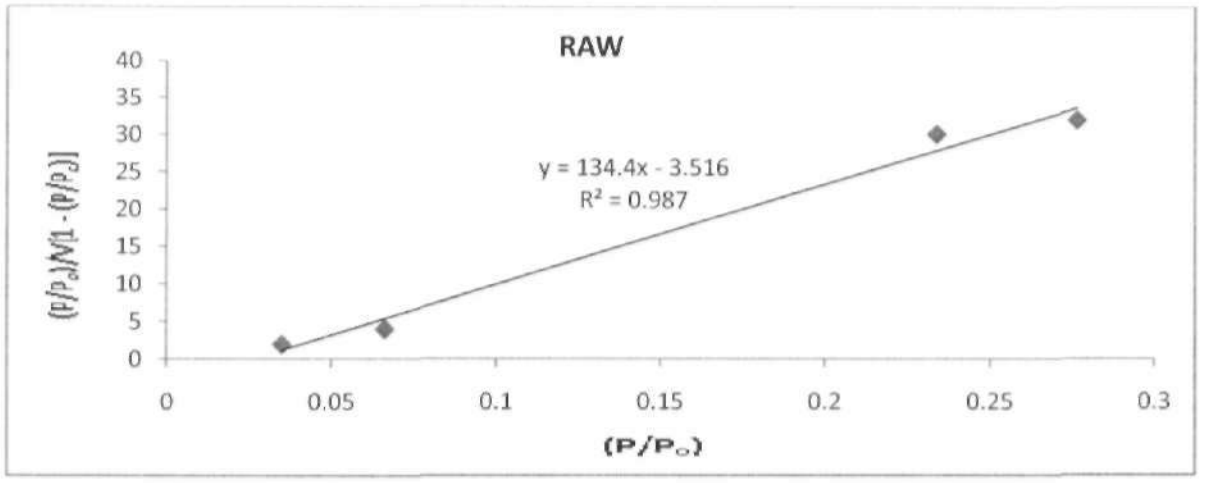
Table B2. BET isotherm of the Bentonite clay samples

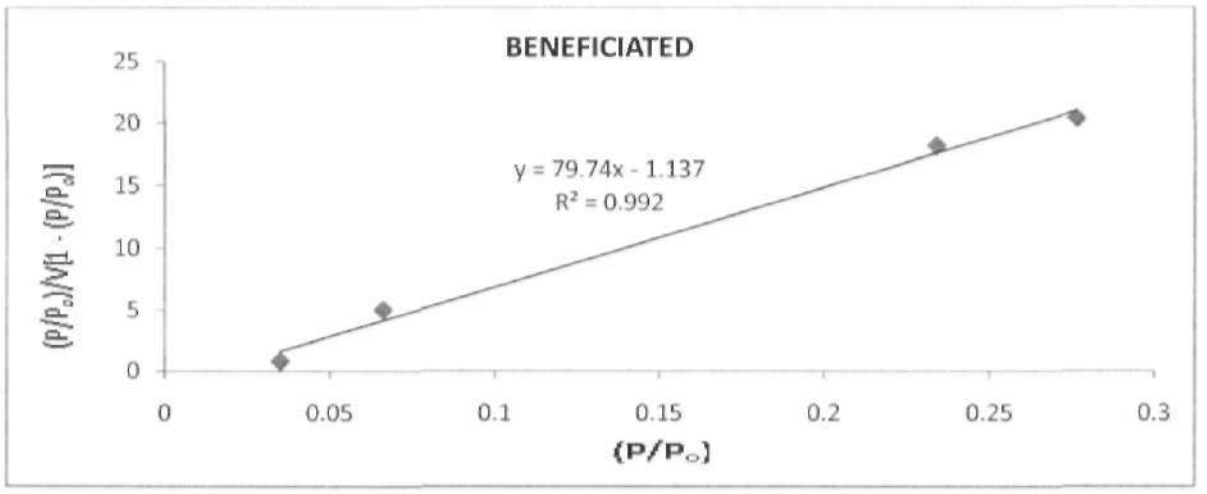
SAMPLE	$CaSO_4$		K_2SO_4		CH_3COONa		$MgCl_2$	
	V (g)	Y (g^{-1})	V (g)	Y (g^{-1})	V (g)	Y (g^{-1})	V (g)	Y (g^{-1})
RAW	0.0181	2.0000	0.0177	4.0000	0.0102	30.0000	0.0119	32.0000
BENEF.	0.0454	0.8000	0.0142	5.0000	0.0169	18.1000	0.0188	20.3000
CALC. 700C	0.0726	0.5000	0.0770	0.9198	0.0401	7.6089	0.0429	8.9011
CALC. 750C	0.0867	0.4186	0.0709	0.9990	0.0418	7.2995	0.0496	7.6987
CALC. 800C	0.0844	0.4300	0.0718	0.9864	0.0562	6.7800	0.0636	4.8000
ACF 700	0.3146	0.1154	0.2551	0.2776	0.0872	3.5000	0.0836	4.5677
ACF 800	0.2919	0.1243	0.2485	0.2850	0.1221	2.4989	0.1157	3.3004
ACF (DRY) 700	0.4660	0.0779	0.3777	0.1875	0.1695	1.8000	0.1554	2.4572
ACF (DRY) 800	0.4369	0.0831	0.3564	0.1987	0.1695	1.8000	0.1801	2.1200

Table B3. BET isotherm of the standards used

STANDARD	$CaSO_4$		K_2SO_4		CH_3COONa		$MgCl_2$	
	V (g)	Y (g^{-1})	V (g)	Y (g^{-1})	V (g)	Y (g^{-1})	V (g)	Y (g^{-1})
A	0.2121	0.17111	0.1021	0.6937	0.0805	3.7892	0.0638	5.9879
B	0.2972	0.1221	0.1238	0.5721	0.0676	4.5108	0.0641	5.9531
C	0.0150	2.4196	0.0052	13.6205	0.0017	179.4806	0.0011	332.15922

Where Y represents $\frac{P/Po}{V(1-P/Po)}$ in Equation (1). Therefore, a plot of Y against P/P_o gives the BET isotherm of each sample as presented in Figure B1 to B4 below.





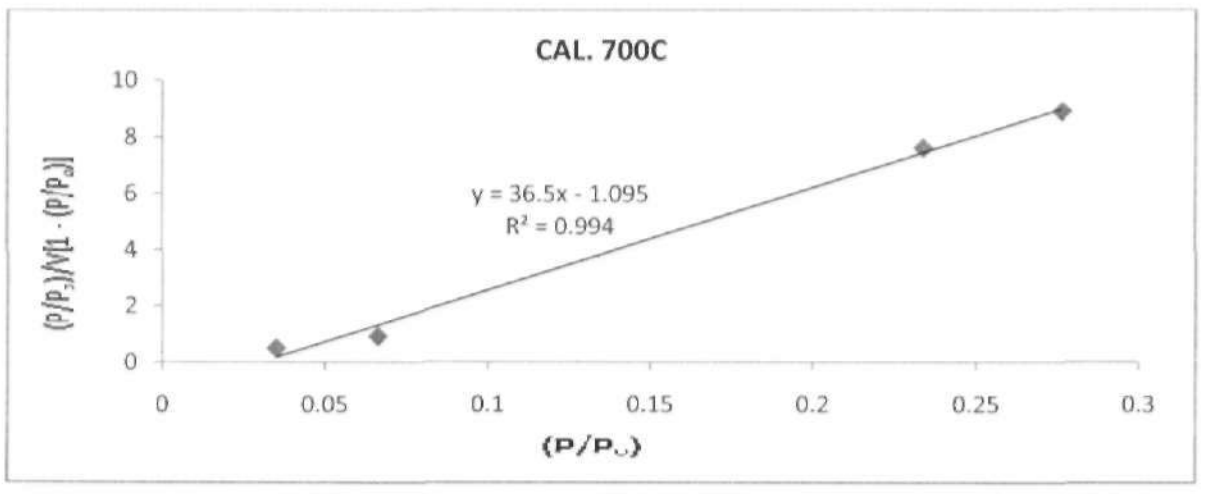


Figure B1. BET isotherm for raw, benaficiated and 700°C calcined clay

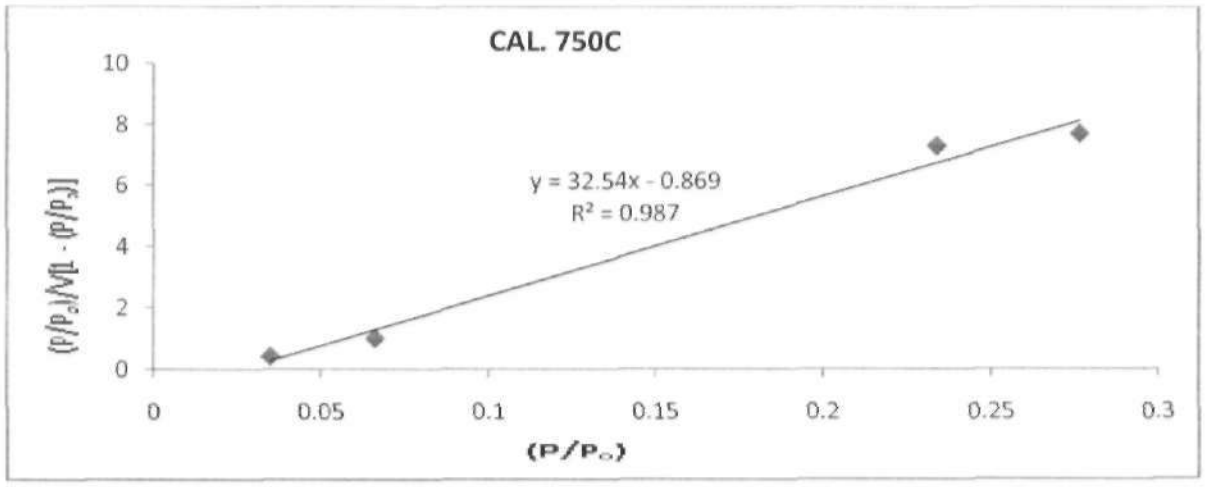
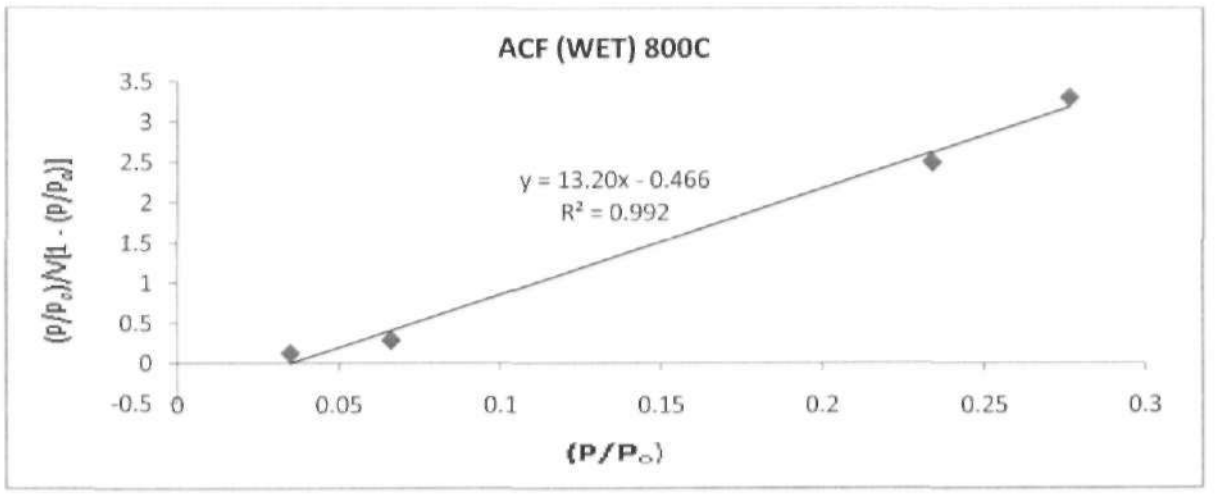
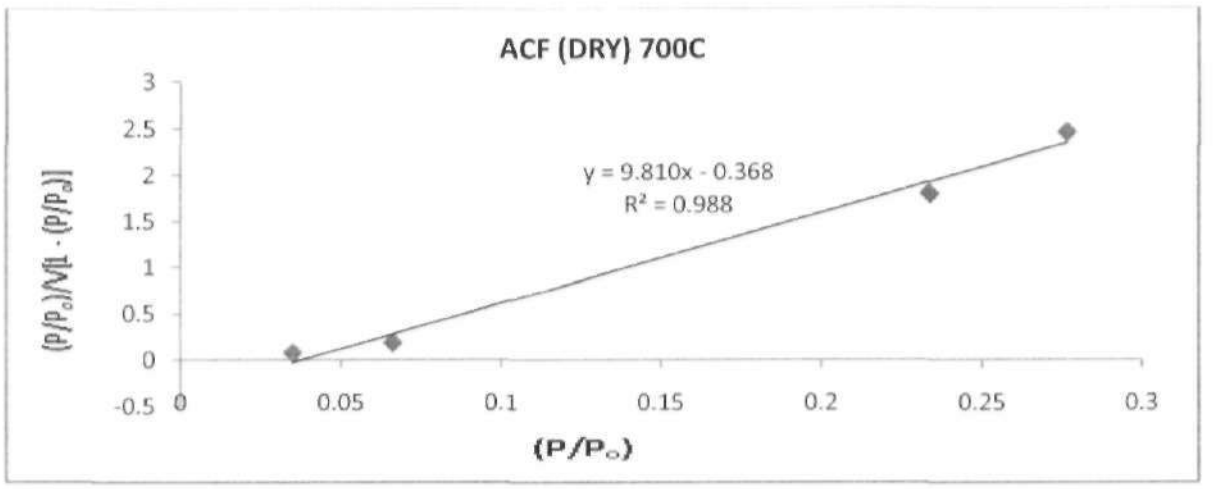


Figure B2. BET isotherm for 700°C, 800°C calcined and 700°C calcined plus wet acdified clay





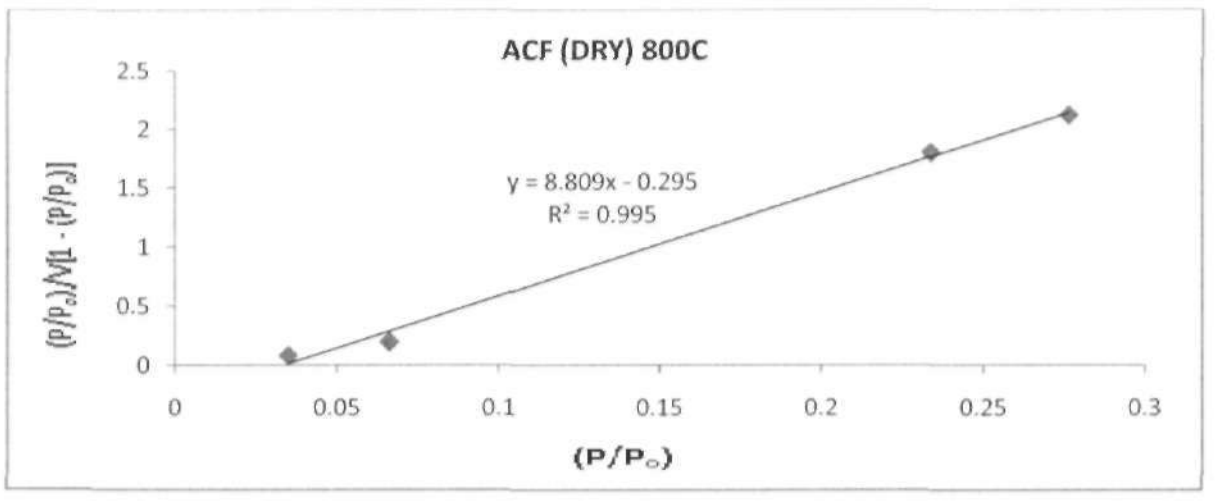
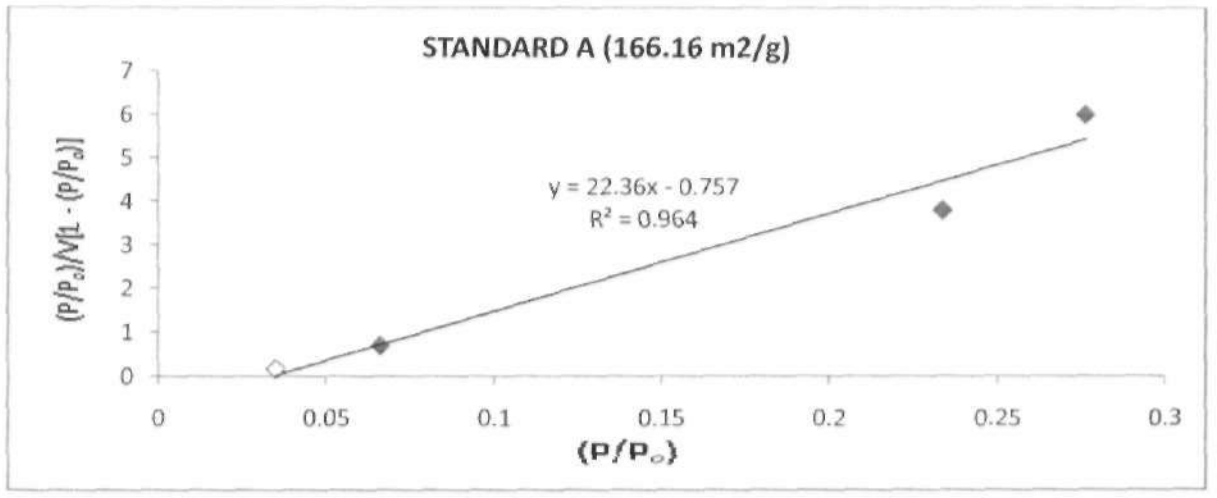
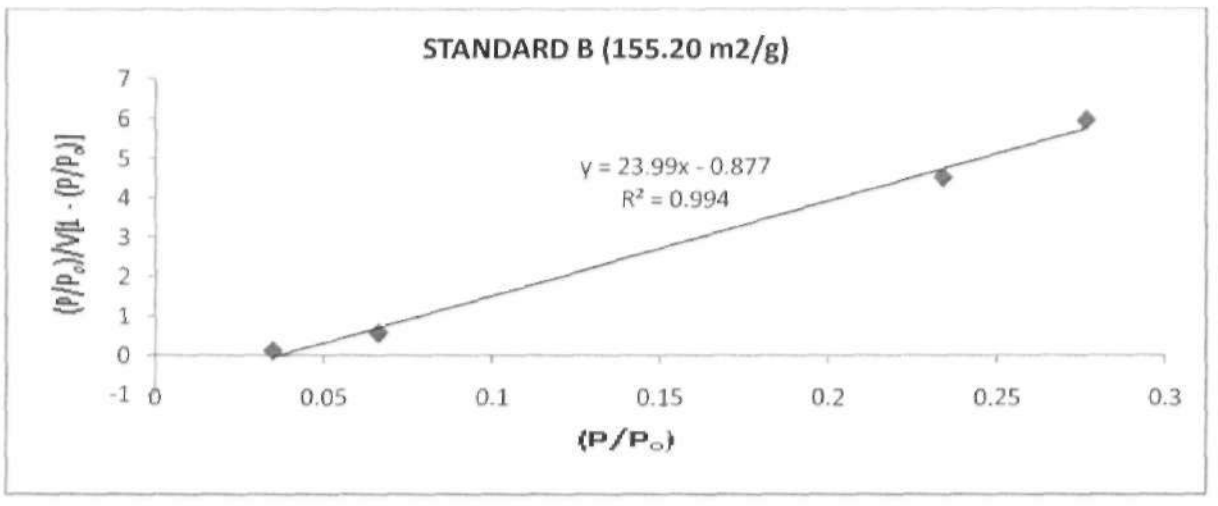


Figure B3. BET isotherm for 800°C plus wet acidified, 700°C and 800°C calcined plus dry acdified clay





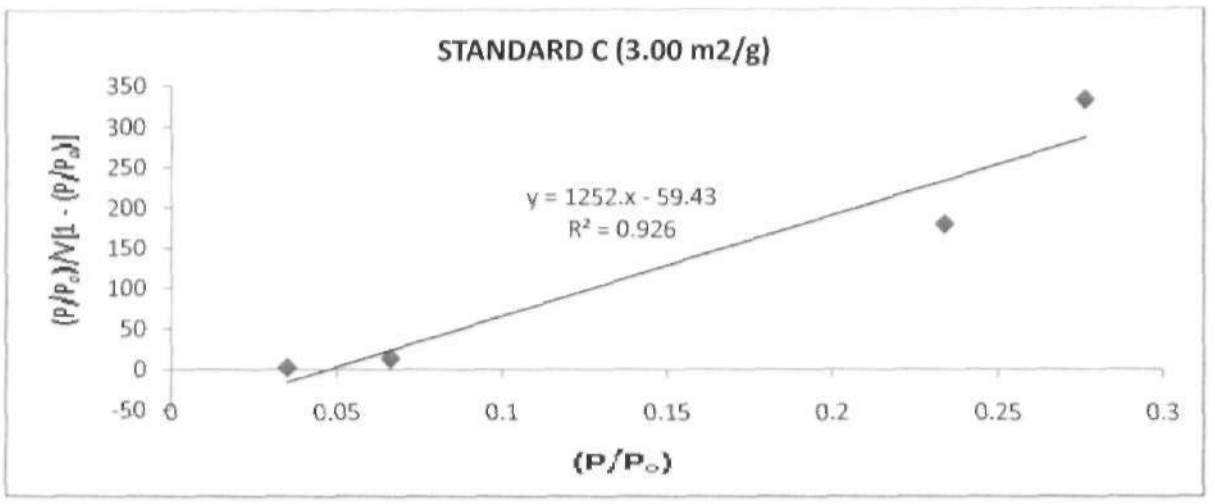


Figure B4. BET isotherm for standards A, B and C.

APPENDIX C

Data for XRD Analysis of Samples

Table C1. XRD data for raw Pindiga clay

PEAK NO.	BRAGG'S ANGLE, 2Θ (°)	d SPACING (Å)	INTENSITY (COUNTS)
1	1.0566	83.5426	6
2	1.3266	66.5399	8
3	1.4816	59.5791	4
4	1.7400	50.7318	5
5	1.9333	45.6598	5
6	2.0383	43.3079	3
7	2.6225	33.6616	10
8	2.8400	31.0841	15
9	3.1400	28.1149	18
10	3.2800	26.9152	20
11	3.5200	25.0806	17
12	3.6800	23.9905	18
13	4.0400	21.8535	7
14	4.3825	20.1464	8
15	4.5225	19.5230	6
16	4.9700	17.7661	2
17	5.1100	17.2797	2

18	5.2600	16.7872	2
19	5.9300	14.8920	6
20	6.4550	13.6819	7
21	6.5600	13.4631	4
22	6.7466	13.0912	4
23	7.0233	12.5760	3
24	7.6600	11.5321	2
25	7.9600	11.0981	4
26	8.2000	10.7738	2
27	8.3500	10.5806	4
28	8.5600	10.3215	2
29	8.9800	9.8397	3
30	9.3038	9.4979	14
31	9.5550	9.2488	3
32	9.7333	9.0798	5
33	9.9600	8.8736	13
34	10.0800	8.7682	13
35	10.7300	8.2385	3
36	11.0750	7.9826	2
37	11.2800	7.8380	2
38	11.5900	7.6290	2
39	11.8800	7.4435	2
40	12.1050	7.3056	3
41	12.3750	7.1468	2
42	12.9050	6.8545	2
43	13.3833	6.6105	4
44	13.6233	6.4946	3
45	13.8500	6.3888	3
46	14.0000	6.3207	2
47	14.2633	6.2046	3
48	14.5100	6.0997	2
49	14.7500	6.0010	4
50	15.0400	5.8859	3
51	15.1500	5.8434	6
52	15.3300	5.7752	5
53	15.5850	5.6813	5
54	15.7550	5.6203	4
55	16.1350	5.4888	4
56	16.3350	5.4221	3
57	16.5050	5.3666	2
58	16.6500	5.3202	4

59	16.9600	5.2236	4
60	17.1400	5.1692	7
61	17.4200	5.0867	10
62	17.8650	4.9610	6
63	18.2400	4.8599	2
64	18.4200	4.8128	8
65	18.5650	4.7755	14
66	19.0950	4.6441	3
67	19.2766	4.6008	3
68	20.0800	4.4185	3
69	20.3783	4.3545	4
70	20.6616	4.2954	4
71	20.9050	4.2459	2
72	21.1483	4.1976	8
73	21.3433	4.1597	5
74	21.6100	4.1090	4
75	21.8400	4.0662	4
76	22.1850	4.0038	2
77	22.3533	3.9740	6
78	22.5500	3.9398	9
79	22.7016	3.9138	10
80	22.9225	3.8766	10
81	23.0833	3.8500	5
82	23.2800	3.8179	2
83	24.0435	3.6983	9
84	24.2000	3.6748	17
85	24.3136	3.6579	60
86	24.5000	3.6304	5
87	25.0375	3.5537	7
88	25.1826	3.5336	10
89	25.4516	3.4968	4
90	25.6483	3.4705	18
91	25.8133	3.4486	4
92	26.0600	3.4166	3
93	26.2050	3.3980	4
94	26.4166	3.3712	5
95	26.8150	3.3220	6
96	26.9733	3.3029	3
97	27.1600	3.2806	3
98	27.7100	3.2167	4
99	27.8650	3.1992	3

100	28.1200	3.1708	2
101	28.2800	3.1532	2
102	28.8200	3.0953	3
103	28.9950	3.0770	2
104	29.2300	3.0528	2
105	29.3733	3.0383	4
106	29.5333	3.0222	4
107	29.8750	2.9884	2
108	30.1150	2.9651	3
109	30.6300	2.9164	2
110	31.0750	2.8757	3
111	31.2750	2.8577	2
112	31.9100	2.8023	2
113	32.0600	2.7895	2
114	32.2750	2.7714	3
115	32.4700	2.7552	5
116	32.6700	2.7388	5
117	32.9550	2.7158	4
118	33.4200	2.6790	5
119	33.5950	2.6655	7
120	33.7833	2.6511	5
121	34.1500	2.6234	8
122	34.4283	2.6029	8
123	34.6400	2.5874	5
124	35.0000	2.5616	2
125	35.3200	2.5392	5
126	36.0100	2.4921	3
127	36.1616	2.4820	4
128	36.5600	2.4558	2
129	36.7350	2.4445	3
130	36.9500	2.4308	3
131	37.1350	2.4191	6
132	37.3700	2.4044	3
133	37.6000	2.3903	3
134	37.7400	2.3817	2
135	37.9966	2.3662	4
136	38.2200	2.3529	2
137	38.5200	2.3353	6
138	38.9100	2.3128	3
139	39.2000	2.2963	3
140	39.6450	2.2716	2

141	39.7950	2.2633	2
142	40.1300	2.2452	3
143	40.5600	2.2224	2
144	40.8600	2.2068	3

Table C2. XRD data for beneficiated Pindiga clay

PEAK NO.	BRAGG'S ANGLE, 2Θ (°)	d SPACING (Å)	INTENSITY (COUNTS)
1	1.1300	78.1162	5
2	1.4150	62.3831	8
3	1.8066	48.8617	3
4	2.0000	44.1370	2
5	2.1425	41.2019	6
6	2.3250	37.9681	5
7	2.6840	32.8904	10
8	2.8200	31.3045	7
9	3.1000	28.4776	13
10	3.2800	26.9152	14
11	3.4925	25.2780	11
12	3.7466	23.5642	10
13	3.9000	22.6377	7
14	4.1100	21.4815	7
15	4.4750	19.7301	3
16	4.7766	18.4850	3
17	5.2250	16.8996	2
18	5.6200	15.7127	3
19	5.8400	15.1213	2
20	6.1333	14.3988	3
21	6.3966	13.8067	5

22	6.6350	13.3111	3
23	6.8000	12.9885	2
24	7.0350	12.5551	3
25	7.3650	11.9933	3
26	7.5900	11.6383	4
27	7.7916	11.3376	4
28	7.9800	11.0703	5
29	8.2633	10.6914	5
30	8.4366	10.4722	5
31	8.7116	10.1422	3
32	9.2875	9.5146	5
33	9.4716	9.3300	7
34	9.7066	9.1047	10
35	9.9466	8.8855	7
36	10.2950	8.5856	3
37	10.4400	8.4667	2
38	10.6550	8.2963	4
39	10.7800	8.2004	3
40	10.9950	8.0405	3
41	11.4250	7.7388	2
42	11.8550	7.4591	3
43	12.0600	7.3328	2
44	12.2733	7.2058	5
45	12.4750	7.0897	3
46	12.6400	6.9976	2
47	12.8350	6.8917	2
48	13.1033	6.7512	3
49	13.2366	6.6835	5
50	13.3800	6.6122	2
51	13.5700	6.5200	3
52	13.7000	6.4584	2
53	13.8700	6.3797	2
54	14.1200	6.2673	2
55	14.2800	6.1974	2
56	14.6100	6.0581	3
57	14.7750	5.9909	3
58	15.0050	5.8995	2
59	15.2700	5.7978	5
60	15.6200	5.6686	3
61	16.0400	5.5211	3
62	16.4600	5.3812	3

63	16.7083	5.3018	3
64	16.9200	5.2359	8
65	17.1000	5.1812	19
66	17.2200	5.1454	23
67	17.6600	5.0181	6
68	17.9125	4.9480	7
69	18.2933	4.8458	14
70	18.5566	4.7776	5
71	18.7266	4.7347	4
72	18.9200	4.6867	2
73	19.2950	4.5964	5
74	19.5100	4.5463	7
75	19.7250	4.4972	2
76	19.9300	4.4514	2
77	20.2100	4.3904	3
78	20.5133	4.3261	4
79	20.7450	4.2783	3
80	20.9650	4.2339	2
81	21.1850	4.1905	4
82	21.4116	4.1466	6
83	21.6366	4.1040	6
84	21.8200	4.0699	4
85	21.9550	4.0452	5
86	22.1600	4.0082	3
87	22.3683	3.9714	10
88	22.5066	3.9473	6
89	22.7400	3.9073	6
90	22.9633	3.8698	7
91	23.2433	3.8238	4
92	23.4850	3.7850	2
93	23.7200	3.7480	2
94	23.9400	3.7141	17
95	24.0812	3.6926	59
96	24.5725	3.6199	6
97	24.8150	3.5851	6
98	24.9950	3.5597	7
99	25.2400	3.5257	4
100	25.3750	3.5072	10
101	25.6650	3.4682	6
102	26.0950	3.4120	3
103	26.2250	3.3954	2

104	26.8800	3.3142	2
105	27.3000	3.2641	2
106	27.5833	3.2312	5
107	27.9500	3.1897	4
108	28.1750	3.1647	4
109	28.3150	3.1494	3
110	28.4450	3.1353	2
111	28.8616	3.09010	5
112	29.1450	3.0615	3
113	29.4000	3.0356	5
114	29.5650	3.0190	2
115	29.9500	2.9811	5
116	30.1600	2.9608	2
117	30.2800	2.9493	2
118	30.5350	2.9253	2
119	30.8483	2.8963	4
120	31.0450	2.8784	4
121	31.2183	2.8628	3
122	31.4500	2.8422	2
123	31.8966	2.8034	5
124	32.1100	2.7853	9
125	32.2830	2.7708	12
126	32.4673	2.7555	11
127	32.6420	2.7411	7
128	32.7850	2.7295	2
129	33.1666	2.6989	4
130	33.4233	2.6788	4
131	33.5900	2.6659	6
132	33.7700	2.6521	6
133	34.0700	2.6294	6
134	34.4133	2.6040	4
135	34.8300	2.5738	4
136	35.0116	2.5608	5
137	35.3266	2.5387	3
138	35.7850	2.5072	4
139	35.9033	2.4992	4
140	36.0600	2.4887	3
141	36.3283	2.4710	4
142	36.8816	2.4352	8
143	37.1850	2.4160	3
144	37.6066	2.3899	3

145	37.8200	2.3769	6
146	38.0000	2.3660	2
147	38.3800	2.3435	2
148	38.6150	2.3297	3
149	39.0533	2.3046	4
150	39.2600	2.2929	2
151	39.6600	2.2707	4
152	39.8950	2.2579	6
153	40.2750	2.2375	3
154	40.5800	2.2213	2
155	40.7700	2.2114	4

Table C3. XRD data for Pindiga clay calcined at 700°C (CAL. 700°C)

PEAK NO.	BRAGG'S ANGLE, 2Θ (°)	d SPACING (Å)	INTENSITY (COUNTS)
1	1.5550	56.7669	2
2	1.8700	47.2052	5
3	2.1433	41.1800	5
4	2.4550	35.9579	2
5	2.7200	32.4552	4
6	3.1000	28.4776	2
7	3.3900	26.0421	3
8	3.5800	24.6604	5
9	3.8700	22.8130	2
10	4.4950	19.6424	4
11	4.8100	18.3567	5
12	5.1416	17.1736	4
13	5.5000	16.0552	6
14	5.5900	15.7969	6
15	5.8000	15.2254	6
16	5.9800	14.7676	9
17	6.3000	14.0182	17
18	6.4800	13.6292	17
19	6.6200	13.3412	14
20	7.5000	11.7777	2
21	7.6550	11.5396	2

22	7.9150	11.1611	3
23	8.1350	10.8600	3
24	8.2600	10.6957	3
25	8.5833	10.2935	4
26	8.8200	10.0178	3
27	9.1556	9.6513	4
28	9.3400	9.4612	2
29	9.5800	9.2247	3
30	9.8300	8.9907	4
31	10.0550	8.7900	2
32	10.4550	8.4546	2
33	10.6566	8.2951	3
34	11.0400	8.0078	4
35	11.3650	7.7796	3
36	11.6966	7.5597	3
37	11.8700	7.4497	2
38	12.2700	7.2077	3
39	12.7100	6.9592	4
40	13.3400	6.6319	4
41	13.5400	6.5344	2
42	13.9400	6.3478	2
43	14.3450	6.1695	2
44	14.5300	6.0913	2
45	14.8800	5.9488	4
46	15.0766	5.8717	4
47	15.3650	5.7621	3
48	15.8200	5.5974	3
49	17.2000	5.1513	20
50	17.4000	5.0925	16
51	17.6000	5.0351	8
52	17.8200	4.9734	3
53	18.1400	4.8864	6
54	18.3000	4.8441	12
55	18.5183	4.7874	6
56	18.7050	4.7401	2
57	18.9416	4.6814	3
58	19.4800	4.5532	5
59	19.8050	4.4792	2
60	20.5800	4.3123	5
61	20.7066	4.2862	3
62	21.0133	4.2243	5

63	21.2750	4.1729	3
64	21.4500	4.1393	3
65	22.0050	4.0361	3
66	22.4000	3.9658	2
67	22.5950	3.9320	3
68	22.8516	3.8885	5
69	23.1800	3.8341	2
70	24.0834	3.6923	66
71	24.3633	3.6505	6
72	24.5550	3.6224	7
73	24.9316	3.5686	13
74	25.2150	3.5291	3
75	25.4150	3.5018	6
76	25.7308	3.4595	5
77	26.7050	3.3355	3
78	27.2200	3.2735	3
79	27.5866	3.2309	4
80	27.8800	3.1975	2
81	28.3400	3.1467	3
82	28.5800	3.1208	3
83	28.9050	3.0864	4
84	29.1600	3.0600	3
85	30.0400	2.9723	2
86	30.2100	2.9560	2
87	30.6450	2.9150	3
88	30.9800	2.8843	3
89	31.7200	2.8186	5
90	31.8350	2.8087	6
91	32.0700	2.7887	7
92	32.3000	2.7693	4
93	32.6450	2.7409	7
94	32.8475	2.7244	5
95	33.1000	2.7042	8
96	33.2866	2.6895	7
97	33.5400	2.6697	4
98	33.9950	2.6350	8
99	34.7000	2.5831	3
100	34.8950	2.5691	3
101	35.1150	2.5535	2
102	35.6600	2.5157	3
103	36.1600	2.4821	3

104	36.6250	2.4516	3
105	36.8700	2.4359	4
106	37.0550	2.4242	2
107	37.2933	2.4092	4
108	37.4750	2.3979	3
109	37.7500	2.3811	3
110	37.8800	2.3732	3
111	38.3600	2.3446	3
112	38.7200	2.3237	2
113	38.8600	2.3156	2
114	39.1633	2.2984	5
115	39.3600	2.2873	2
116	39.5700	2.2757	3
117	39.8900	2.2582	6
118	40.1600	2.2436	4

Table C4. XRD data for Pindiga clay calcined at 750°C (CAL. 750°C)

PEAK NO.	BRAGG'S ANGLE, 2Θ (°)	d SPACING (Å)	INTENSITY (COUNTS)
1	1.2950	68.1635	2
2	1.7600	50.1553	2
3	1.9750	44.6958	2
4	2.5050	35.2403	2
5	3.2450	27.2055	5
6	3.4750	25.4050	2
7	3.7000	23.8609	5
8	3.8800	22.7543	13
9	4.0400	21.8535	15
10	4.5250	19.5122	3
11	4.7400	18.6277	3
12	5.0300	17.5543	2
13	5.2700	16.7554	2
14	5.4966	16.0652	6
15	5.7333	15.4024	4
16	5.9500	14.8419	7
17	6.1400	14.3831	11
18	6.3000	14.0182	12
19	6.5000	13.5873	8
20	6.7400	13.1040	5

21	6.9466	12.7147	3
22	7.3600	12.0014	3
23	7.7200	11.4426	4
24	8.0700	10.9471	2
25	8.2600	10.6957	5
26	8.5800	10.2975	3
27	8.7200	10.1325	3
28	8.9216	9.9040	4
29	9.2650	9.5376	3
30	9.6466	9.1612	9
31	10.7000	8.2615	2
32	10.9400	8.0808	4
33	11.1300	7.9433	4
34	11.5366	7.6642	4
35	11.6900	7.5640	2
36	11.8600	7.4560	3
37	12.3800	7.1439	2
38	12.6950	6.9674	2
39	13.3350	6.6344	3
40	13.6400	6.4867	3
41	14.0450	6.3006	3
42	14.2400	6.2147	3
43	14.6866	6.0267	4
44	14.9000	5.9409	3
45	15.1750	5.8338	2
46	15.4433	5.7331	5
47	15.7000	5.6399	4
48	15.8450	5.5886	2
49	16.0600	5.5143	2
50	16.4300	5.3909	2
51	16.8000	5.2730	3
52	17.0000	5.2114	9
53	17.2200	5.1454	21
54	17.5600	5.0465	8
55	17.7433	4.9948	5
56	17.9450	4.9391	2
57	18.2500	4.8572	12
58	18.6600	4.7514	3
59	18.9850	4.6708	4
60	19.1900	4.6214	2
61	19.4450	4.5613	5

62	19.5900	4.5279	4
63	19.7700	4.4871	2
64	19.9866	4.4389	4
65	20.1600	4.4011	5
66	20.5200	4.3247	4
67	20.6800	4.2916	5
68	20.8800	4.2510	4
69	21.6150	4.1081	3
70	21.9450	4.0470	4
71	22.4250	3.9615	6
72	22.7666	3.9028	7
73	23.0000	3.8637	6
74	23.5200	3.7795	3
75	23.8400	3.7294	9
76	24.0300	3.7004	70
77	24.4650	3.6356	7
78	24.9150	3.5709	12
79	25.1633	3.5362	6
80	25.4200	3.5011	6
81	25.9000	3.4373	2
82	26.8000	3.3239	4
83	26.9750	3.3027	4
84	27.4900	3.2420	4
85	27.6000	3.2293	3
86	27.8100	3.2054	2
87	28.1100	3.1719	4
88	28.4200	3.1380	4
89	29.3450	3.0411	2
90	29.9100	2.9850	2
91	31.3800	2.8484	3
92	31.6950	2.8208	8
93	31.8350	2.8087	7
94	32.0033	2.7943	5
95	32.2400	2.7744	5
96	32.4700	2.7552	8
97	32.7000	2.7364	3
98	32.9800	2.7138	6
99	33.1400	2.7010	7
100	33.3500	2.6845	2
101	33.6400	2.6620	2
102	33.9400	2.6392	9

103	34.0800	2.6287	2
104	34.2500	2.6150	2
105	34.4850	2.5987	2
106	35.0200	2.5602	5
107	35.2266	2.5457	4
108	35.9050	2.4991	3
109	36.1000	2.4861	4
110	36.6650	2.4490	2
111	36.9000	2.4340	7
112	37.1700	2.4169	3
113	37.3550	2.4054	3
114	37.6000	2.3903	5
115	37.8600	2.3744	6
116	38.1200	2.3588	2
117	38.7150	2.3240	4
118	38.9600	2.3099	4
119	39.2250	2.2949	3
120	39.4450	2.2826	3
121	39.8300	2.2614	5
122	40.0300	2.2506	3
123	40.5000	2.2255	2

Table C5. XRD data for Pindiga clay calcined at 800°C (CAL. 800°C)

PEAK NO.	BRAGG'S ANGLE, 2Θ (°)	d SPACING (Å)	INTENSITY (COUNTS)
1	1.2666	69.6918	4
2	1.9366	45.5820	3
3	2.2900	38.5484	5
4	2.5700	34.3491	7
5	2.9050	30.3887	3
6	3.1316	28.1903	4
7	3.4450	25.6265	6
8	3.7933	23.2742	3
9	3.9666	22.2577	5
10	4.4600	19.7965	5
11	4.7000	18.7861	4
12	4.9800	17.7305	3
13	5.1750	17.0628	3
14	5.3433	16.5257	4

15	5.5150	16.0116	3
16	5.8800	15.0185	7
17	6.0600	14.5728	10
18	6.3200	13.9738	19
19	6.5400	13.5043	12
20	6.7100	13.1625	9
21	6.8400	12.9126	5
22	7.5266	11.7362	3
23	7.6450	11.5547	3
24	7.9950	11.0496	4
25	8.8200	10.0178	3
26	9.0900	9.7208	3
27	9.4000	9.4010	4
28	9.8916	8.9348	4
29	10.1850	8.6781	3
30	10.4750	8.4385	3
31	10.6533	8.2976	7
32	10.8350	8.1589	3
33	11.1400	7.9362	5
34	11.5200	7.6752	4
35	11.9700	7.3877	3
36	12.1950	7.2519	4
37	12.3000	7.19021	4
38	12.7000	6.9646	3
39	13.1400	6.7324	3
40	13.6200	6.4962	3
41	14.1000	6.2761	5
42	14.3983	6.1467	9
43	14.5800	6.0705	6
44	14.8000	5.9808	4
45	15.0016	5.9009	5
46	15.4200	5.7417	4
47	15.5600	5.6903	4
48	15.7150	5.6346	3
49	15.9000	5.5694	3
50	17.0000	5.2114	9
51	17.1200	5.1752	16
52	17.2800	5.1276	19
53	17.4400	5.0809	17
54	17.6200	5.0294	5
55	17.7933	4.9808	5

56	18.2725	4.8513	19
57	18.5775	4.7723	7
58	18.9150	4.6879	3
59	19.0550	4.6538	5
60	19.8100	4.4781	4
61	19.9666	4.4433	5
62	20.3300	4.3647	4
63	20.5980	4.3085	8
64	20.9116	4.2446	5
65	21.4200	4.1450	4
66	21.5200	4.1260	3
67	21.6600	4.0996	4
68	22.2000	4.0011	3
69	22.5900	3.9329	5
70	22.6950	3.9149	6
71	22.9283	3.8756	8
72	23.1133	3.8450	11
73	23.4300	3.7938	6
74	23.7800	3.7387	11
75	24.0477	3.6977	86
76	24.4883	3.6322	8
77	24.7250	3.5979	11
78	24.8616	3.5785	13
79	25.1000	3.5450	5
80	25.2750	3.5209	5
81	25.4933	3.4912	3
82	25.7083	3.4625	4
83	25.8500	3.4438	4
84	26.1066	3.4106	3
85	26.4600	3.3658	4
86	26.9100	3.3105	6
87	27.4200	3.2501	5
88	27.5200	3.2385	5
89	27.6925	3.2187	6
90	27.8700	3.1986	5
91	28.2900	3.1521	8
92	28.5000	3.1294	6
93	28.6850	3.1096	4
94	29.0900	3.0672	3
95	30.1900	2.9579	3
96	30.6400	2.9155	6

97	30.8033	2.9004	6
98	31.0050	2.8820	7
99	31.2550	2.8595	3
100	31.4600	2.8413	8
101	31.6150	2.8278	5
102	31.7400	2.8169	3
103	31.9683	2.7973	7
104	32.2000	2.7777	4
105	32.3950	2.7614	4
106	32.9100	2.7194	8
107	33.1216	2.7025	7
108	33.3100	2.6876	4
109	33.6350	2.6624	3
110	33.9000	2.6422	3
111	34.0250	2.6328	7
112	34.3200	2.6108	3
113	35.3285	2.5386	3
114	36.0700	2.4881	4
115	36.6950	2.4471	3
116	36.8950	2.4343	6
117	37.0666	2.4234	4
118	37.2400	2.4125	3
119	37.7283	2.3824	8
120	37.9200	2.3708	5
121	38.2800	2.3494	3
122	39.7750	2.2644	3
123	39.9150	2.2568	5
124	40.1900	2.2420	3
125	40.4800	2.2266	3
126	40.8300	2.2083	7

Table C6. XRD data for Pindiga clay calcined at 700°C and wet acidified [ACF (WET) 700°C]

PEAK NO.	BRAGG'S ANGLE, 2Θ (°)	d SPACING (Å)	INTENSITY (COUNTS)
1	1.34830	65.4690	5
2	2.7200	32.4552	4
3	3.4350	25.7010	4
4	3.6200	24.3880	5

5	5.6240	15.7015	6
6	5.7383	15.3890	4
7	5.9200	14.9171	4
8	6.1575	14.3422	6
9	6.4400	13.7137	5
10	6.6600	13.2612	8
11	7.2783	12.1360	4
12	7.9650	11.0911	6
13	8.7550	10.0920	4
14	8.9400	9.8836	14
15	9.0936	9.7170	129
16	9.4016	9.3994	5
17	9.8466	8.9755	5
18	9.9850	8.8514	4
19	11.0766	7.9815	5
20	11.2625	7.8501	7
21	11.4250	7.7388	8
22	11.7633	7.5170	6
23	12.2533	7.2175	5
24	13.1816	6.7112	5
25	14.7733	5.9915	6
26	15.3225	5.7780	6
27	15.8000	5.6044	4
28	17.5200	5.0579	12
29	18.1620	4.8805	11
30	18.3206	4.8387	23
31	18.7100	4.7388	5
32	19.0766	4.6486	5
33	19.2475	4.6077	5
34	19.6666	4.510	4
35	19.8967	4.4588	5
36	20.2025	4.3920	6
37	21.0250	4.2220	7
38	21.9275	4.0502	5
39	22.0440	4.0291	7
40	22.3666	3.9717	4
41	22.7860	3.8995	8
42	23.4660	3.7880	5
43	23.5983	3.7671	7
44	23.9400	3.7141	11
45	24.1160	3.6874	82

46	24.4166	3.6427	2
47	24.9802	3.5617	18
48	25.4255	3.5004	15
49	25.8150	3.4484	6
50	26.2933	3.3868	5
51	26.5558	3.3539	7
52	27.0350	3.2955	7
53	27.3200	3.2618	7
54	27.5550	3.2345	9
55	27.6965	3.2183	8
56	28.2626	3.1551	11
57	28.4616	3.1335	6
58	28.8800	3.0890	6
59	30.3950	2.9384	14
60	30.7266	2.9075	4
61	30.8766	2.8937	5
62	31.0500	2.8779	4
63	31.1875	2.8655	5
64	31.7225	2.8184	6
65	32.0166	2.7932	9
66	32.3200	2.7677	6
67	32.5625	2.7476	10
68	33.4150	2.6794	6
69	33.6525	2.6611	6
70	33.9700	2.6369	7
71	34.1000	2.6272	4
72	34.9583	2.56460	5
73	35.2467	2.5443	4
74	35.4950	2.5270	5
75	35.9133	2.4986	4
76	36.1116	2.4853	7
77	36.7116	2.4460	4
78	36.9225	2.4326	8
79	37.2133	2.4142	4
80	37.6550	2.3869	4
81	39.2225	2.2950	5
82	39.8666	2.2594	7
83	39.9800	2.2533	6
84	40.2000	2.2415	5
85	40.8808	2.2057	5

Table C7. XRD data for Pindiga clay calcined at 800°C and wet acidified [ACF (WET) 800°C]

PEAK NO.	BRAGG'S ANGLE, 2Θ (°)	d SPACING (Å)	INTENSITY (COUNTS)
1	1.2566	70.2464	4
2	1.5800	55.8688	4
3	1.9200	45.9761	8
4	2.0733	42.5769	5
5	2.2100	39.9436	5
6	2.3383	37.7522	8
7	2.6900	32.8171	8
8	2.7800	31.7549	4
9	3.1433	28.0854	4
10	3.2950	26.7927	2
11	3.8800	22.7543	8
12	4.0000	22.0720	7
13	5.0750	17.3988	3
14	5.9100	14.9423	4
15	6.2100	14.2211	8
16	7.1033	12.4346	5
17	7.3300	12.0505	3
18	7.4533	11.8514	5
19	8.0200	11.0152	4
20	8.3700	10.5554	3
21	8.6400	10.2261	3
22	9.0200	9.7961	2
23	9.3600	9.4410	6
24	9.7000	9.1109	4
25	9.8500	8.9725	4
26	10.3550	8.5360	4
27	10.5366	8.3893	4
28	10.6550	8.2963	2
29	10.9133	8.1005	4
30	11.0850	7.9754	9
31	11.3400	7.7967	7
32	11.6450	7.5931	2
33	12.1150	7.2996	5
34	12.2966	7.1922	5
35	12.5783	7.0317	4

36	12.8800	6.8677	2
37	13.3283	6.6377	3
38	13.5083	6.5497	3
39	15.3200	5.7789	4
40	16.0450	5.5194	2
41	16.2550	5.4486	4
42	16.5483	5.3527	4
43	16.7266	5.2960	3
44	17.1800	5.1572	34
45	17.3000	5.1217	44
46	17.5000	5.0637	25
47	17.7400	4.9957	26
48	17.9800	4.9295	18
49	19.6600	4.5119	9
50	19.8193	4.4760	14
51	19.9962	4.4368	14
52	20.1833	4.3961	10
53	20.3420	4.3622	8
54	21.6033	4.1102	17
55	21.8965	4.0559	6
56	22.5690	3.9365	5
57	22.7306	3.9089	9
58	22.8600	3.8871	9
59	22.9800	3.8670	9
60	23.2300	3.8260	3
61	24.1008	3.6897	62
62	24.6375	3.6105	10
63	24.9250	3.5695	16
64	25.0600	3.5506	8
65	25.2140	3.5292	5
66	25.3350	3.5127	6
67	25.4800	3.4930	4
68	25.6933	3.4645	3
69	26.3233	3.3830	7
70	26.6750	3.3392	2
71	26.9400	3.3069	7
72	27.2898	3.2653	6
73	27.5200	3.2385	2
74	28.0416	3.1795	7
75	28.1850	3.1636	3
76	28.4250	3.1374	2

77	28.6300	3.1154	5
78	29.0450	3.0719	2
79	29.4066	3.0349	3
80	29.6316	3.0124	4
81	30.0000	2.9762	2
82	30.1283	2.9638	5
83	30.8700	2.8943	3
84	31.5525	2.8332	7
85	31.7175	2.8189	7
86	32.2850	2.7706	8
87	32.4683	2.7554	10
88	32.6466	2.7407	5
89	32.8075	2.7277	9
90	33.0413	2.7089	10
91	33.4820	2.6742	11
92	33.7225	2.6557	6
93	33.9100	2.6414	5
94	34.2850	2.6134	2
95	34.4750	2.5994	2
96	34.6400	2.5874	3
97	34.9350	2.5663	6
98	35.4525	2.5300	9
99	35.7200	2.5116	3
100	35.8650	2.5018	2
101	36.0566	2.4890	5
102	36.1975	2.4796	6
103	36.9366	2.4317	10
104	37.1366	2.4190	6
105	37.3133	2.4080	9
106	37.6800	2.3854	3
107	37.9300	2.3702	2
108	38.0950	2.3603	4
109	38.2750	2.3496	2
110	38.4650	2.3385	2
111	39.0100	2.3071	8
112	39.1650	2.2983	4
113	39.3283	2.2891	6
114	39.8500	2.2603	7
115	40.0150	2.2514	6
116	40.1600	2.2436	6
117	40.3546	2.2332	10

118	40.5200	2.2245	3
119	40.7300	2.2135	3

Table C8. XRD data for Pindiga clay calcined at 700°C and dry acidified [ACF (DRY) 700°C]

PEAK NO.	BRAGG'S ANGLE, 2Θ (°)	d SPACING (Å)	INTENSITY (COUNTS)
1	1.3800	63.9652	2
2	1.6100	54.8278	2
3	2.3150	38.1321	4
4	2.6700	33.0629	3
5	2.9100	30.3366	2
6	3.5400	24.9390	3
7	3.6400	24.2541	3
8	3.9600	22.2948	13
9	4.4000	20.0663	3
10	4.7600	18.5494	3
11	5.4550	16.1876	3
12	6.0300	14.6452	7
13	6.2300	14.1755	8
14	6.4400	13.7137	5
15	6.8800	12.8376	3
16	7.6800	11.5021	4
17	8.0450	10.9810	6
18	8.2800	10.6700	2
19	8.7800	10.0630	2
20	9.3600	9.4410	6
21	9.7050	9.1062	13
22	10.1000	8.7509	2
23	10.3600	8.5319	2
24	10.9100	8.1030	7
25	11.1625	7.9202	6
26	11.8300	7.4748	4
27	12.2100	7.2430	2
28	12.4800	7.08691	2
29	12.8050	6.9078	3
30	13.2100	6.6969	2
31	13.5750	6.5176	5

32	13.7500	6.4351	3
33	14.0000	6.3207	3
34	14.2500	6.2104	3
35	14.6300	6.0499	3
36	14.9500	5.9211	3
37	15.1600	5.8396	3
38	15.5900	5.6795	3
39	16.4450	5.3861	3
40	16.7200	5.2981	2
41	16.9200	5.2359	15
42	17.1346	5.1708	46
43	17.5600	5.0465	23
44	17.8800	4.9569	18
45	18.1600	4.8811	15
46	18.4333	4.8093	8
47	18.8900	4.6941	5
48	19.2400	4.6095	3
49	19.4200	4.5671	2
50	19.7166	4.4991	6
51	20.0966	4.4149	9
52	20.8866	4.2496	4
53	21.1750	4.1924	3
54	21.4700	4.1355	9
55	21.7566	4.0816	4
56	22.1250	4.0145	7
57	22.4800	3.9519	4
58	22.7883	3.8991	11
59	23.1150	3.8447	3
60	23.5800	3.7700	4
61	23.9803	3.7079	51
62	24.3000	3.6599	3
63	24.4600	3.6363	3
64	24.8000	3.5872	18
65	24.9600	3.5646	5
66	25.4050	3.5031	5
67	25.5600	3.4822	2
68	26.2050	3.3980	3
69	26.7550	3.3293	2
70	27.4900	3.2420	5
71	27.8400	3.2020	2
72	28.1050	3.1724	4

73	28.2800	3.1532	3
74	28.6200	3.1165	4
75	28.8066	3.0967	4
76	29.4700	3.0285	3
77	29.8300	2.9928	3
78	31.2450	2.8604	2
79	31.4300	2.8440	2
80	32.0300	2.7921	4
81	32.3900	2.7619	3
82	32.9800	2.7138	4
83	33.3100	2.6876	6
84	33.5433	2.6695	3
85	33.8700	2.645	8
86	34.1033	2.6269	3
87	34.3500	2.6086	4
88	34.9050	2.5684	2
89	35.1383	2.5519	3
90	35.8000	2.5062	4
91	36.2000	2.4794	2
92	36.5300	2.4578	5
93	36.7400	2.4442	5
94	36.9400	2.4314	5
95	37.1800	2.4163	2
96	37.5150	2.3955	2
97	37.7400	2.3817	3
98	38.1500	2.3571	2
99	38.5400	2.3341	3
100	39.1500	2.2991	3
101	39.8900	2.2582	2
102	40.1000	2.2468	3
103	40.6050	2.2200	2

Table C9. XRD data for Pindiga clay calcined at 800°C and dry acidified [ACF (DRY) 800°C]

PEAK NO.	BRAGG'S ANGLE, 2Θ (°)	d SPACING (Å)	INTENSITY (COUNTS)
1	1.2950	68.1635	2
2	1.8050	48.9050	2
3	2.0200	43.7002	2

4	2.2400	39.4087	6
5	2.4450	36.1049	3
6	2.7300	32.3364	6
7	2.9100	30.3366	2
8	3.2900	26.8334	5
9	3.7600	23.4802	8
10	4.2000	21.0213	3
11	4.4750	19.7301	3
12	4.6750	18.8860	3
13	4.9750	17.7483	3
14	5.2200	16.9158	4
15	5.4150	16.3071	3
16	5.6200	15.7127	5
17	5.8000	15.2254	3
18	6.0000	14.7184	7
19	6.1200	14.4300	8
20	6.4400	13.7137	9
21	6.6800	13.2215	10
22	6.8700	12.8563	6
23	7.0433	12.5404	5
24	7.3250	12.0587	4
25	7.5700	11.6690	5
26	7.7800	11.3545	3
27	7.9400	11.1260	2
28	8.3566	10.5723	4
29	8.7400	10.1093	2
30	9.1600	9.6467	17
31	9.3966	9.4043	4
32	9.6200	9.1865	2
33	9.9400	8.8914	4
34	10.4100	8.4910	2
35	10.7300	8.2385	7
36	11.1400	7.9362	6
37	11.5083	7.6830	8
38	11.7516	7.5245	4
39	11.9650	7.3908	2
40	12.2150	7.2401	2
41	12.8100	6.9051	2
42	13.2716	6.6659	3
43	13.4850	6.5609	2
44	13.7000	6.4584	3

45	13.9000	6.3660	2
46	14.0850	6.2828	3
47	14.8800	5.9488	2
48	15.0600	5.8781	5
49	15.2866	5.7915	4
50	15.5150	5.7067	5
51	15.7700	5.6150	3
52	15.9400	5.5556	4
53	16.9400	5.2298	3
54	17.2000	5.1513	14
55	17.4400	5.0809	17
56	17.6600	5.0181	9
57	17.7800	4.9845	8
58	18.0200	4.9187	3
59	18.2400	4.8599	15
60	18.3600	4.8284	12
61	18.6266	4.7598	4
62	19.2450	4.6083	3
63	19.4480	4.5606	6
64	19.6100	4.5233	4
65	19.9000	4.4580	4
66	20.1400	4.4055	3
67	20.7350	4.2804	7
68	20.8850	4.2500	8
69	21.4350	4.1421	6
70	21.6800	4.0959	4
71	21.9350	4.0488	6
72	22.1200	4.0154	4
73	22.3000	3.9834	4
74	22.6350	3.9252	4
75	22.7600	3.9039	4
76	22.9243	3.8763	14
77	23.1366	3.8412	7
78	23.2400	3.8244	6
79	23.3966	3.7991	4
80	23.8600	3.7264	5
81	24.1227	3.6864	82
82	24.3800	3.6480	4
83	24.6300	3.6116	6
84	24.8800	3.5759	12
85	25.0050	3.5583	17

86	25.4833	3.4925	8
87	25.9950	3.4249	3
88	26.1700	3.4024	2
89	26.5200	3.3583	2
90	26.6600	3.3410	4
91	27.0266	3.2965	4
92	27.3166	3.2622	5
93	27.6500	3.2236	3
94	27.7933	3.2073	4
95	28.1900	3.1631	5
96	28.3900	3.1412	3
97	28.5650	3.1224	3
98	28.7250	3.1053	3
99	28.9250	3.0843	5
100	29.1300	3.0631	2
101	29.3400	3.0416	2
102	29.6300	3.0125	5
103	29.9400	2.9820	3
104	30.1133	2.9653	5
105	30.4733	2.9311	5
106	30.6550	2.9141	2
107	30.9200	2.8897	2
108	31.2100	2.8635	3
109	31.7350	2.8173	3
110	31.9433	2.7994	4
111	32.1550	2.7815	5
112	32.3400	2.7660	3
113	32.5400	2.7495	3
114	32.7200	2.7347	3
115	33.0000	2.7122	4
116	33.1816	2.6977	3
117	33.3500	2.6845	6
118	33.5350	2.6701	2
119	34.0850	2.6283	5
120	34.4900	2.5983	3
121	34.6900	2.5838	5
122	35.1100	2.5539	3
123	35.4100	2.5329	5
124	35.5866	2.5207	4
125	35.9950	2.4931	3
126	36.1600	2.4821	4

127	36.3450	2.4699	2
128	36.9600	2.4302	6
129	37.7050	2.3838	2
130	37.9450	2.3693	2
131	38.2150	2.3532	2
132	38.6750	2.3263	3
133	38.8600	2.3156	2
134	39.1850	2.2972	5
135	39.4000	2.2851	5
136	39.9400	2.2555	6
137	40.1200	2.2457	3
138	40.3150	2.2353	4
139	40.8850	2.2055	3